CATALYTIC HYDRODEHALOGENATIVE COUPLING OF DICHLORODIFLUOROMETHANE ON SUPPORTED PLATINUM AND PALLADIUM BIMETALLIC CATALYSTS

by

Debasish Chakraborty

B.S., Bangladesh University of Engineering & Technology, 1998

Submitted to the Graduate Faculty of

School of Engineering in partial fulfillment

of the requirements for the degree of

Master of Science

University of Pittsburgh

2002

UNIVERSITY OF PITTSBURGH

SCHOOL OF ENGINEERING

This thesis was presented

by

Debasish Chakraborty

It was defended on

November 25, 2002

and approved by

Julie L. d'Itri, Associate Professor, Department of Chemical & Petroleum Engineering

Vladimir I. Kovalchuk, Research Professor, Department of Chemical & Petroleum Engineering

Irving Wender, Professor, Department of Chemical & Petroleum Engineering

Thesis Advisor:Julie L. d'Itri, Associate Professor, Department of Chemical & Petroleum Engineering

ABSTRACT

CATALYTIC HYDRODEHALOGENATIVE COUPLING OF DICHLORODIFULORMETHANE ON SUPPORTED PLATINUM AND PALLADIUM BIMETALLIC CATALYSTS

Debasish Chakraborty, M.S.

University of Pittsburgh, 2002

Ethylene and propylene are very important chemicals used as feedstocks in modern days. Halocarbons can be a promising starting material to form C-C coupling products. The biggest challenge of forming coupling products from chlorofluorocarbons (CFCs) is to improve the coupling pathways by suppressing other paths of reactions that produce less attractive products. The kinetics results of the reaction of CF_2Cl_2 and H_2 catalyzed by PtCu/C catalysts, presented in Chapter 3, showed the effect of Cu content on the selectivity pattern. The observation was that the coupling selectivity increased with the increasing Cu content. Chapter 4 discusses the results of introducing CO in the reaction mixture. The maximum coupling selectivity was increased from 55% to 69%. The catalyst was also exposed to water for better mixing of the precursors. The water-exposed catalyst showed an overall coupling selectivity of ~82% and the performance was very stable. It was suggested that water exposure of the fresh catalyst increased bimetallic particle formation. As a result the number and size of Pt particles decreased. Both the results point toward fact that Pt or bimetallic sites may be responsible for C_1 product formation and Cu sites are responsible for coupling products formation. The performances of the palladium

bimetallic catalysts were discussed in chapter 5. Monometallic Pd produced 75% hydrocarbon oligomerization products (C_2 to C_5). For Pd-Ag/C catalyst, there might be a very significant amount of bimetallic particle formation and Ag segregates hugely to the surface of the bimetallic particles. The hydrodehalogenation and coupling reactions are occurring over the Ag sites. For Pd-Cu there will be a moderate surface segregation of Cu to the surface and there will be just enough Pd surface atoms to dissociate hydrogen to Cu sites for dehalogenation and coupling. For Pd-Co/C, the function of Co is just to dilute the Pd ensemble. For Pd-Fe, Fe acts as Pd site blocking and Pd ensemble size reducing element. Two of the bimetallic catalysts (Pd-Cu and Pd-Co) were very stable though their activities were lower than monometallic Pd.

FOREWARD

I am thankful to all the people who have helped me directly or indirectly to finish the work. First of all I would like to thank my advisor Professor Julie L. d'Itri for her advice, guidance and help throughout the research work. I would like to express my sincere gratitude toward Professor Vladimir I. Kovalchuk for his close supervision and guidance. This work was not possible without his help. I express my wholehearted appreciation to Dr. Parag Kulkarni, who passed me the torch of halocarbon research. I am also thankful to my committee member Professor Irving Wender for reviewing my work.

I would like to thank our group members: Mr. Vladimir Pushkarev and Dr. Alex Kudryashev for their helping hands.

My Special thanks to Professor Vladimir Zaikovoskii for the TEM images. Funding from the National Science Foundation is gratefully acknowledged.

TABLE OF CONTENTS

Page

Page

LIST OF TABLES

Page

LIST OF FIGURES

Page

Page

Page

1.0 INTRODUCTION

1.1 Importance of C-C Coupling

Carbon-carbon coupling products like ethylene and propylene have diverse application as feedstock for industries. Ethylene is the largest volume building block for many petrochemicals. It is the most significant organic chemical produced today in terms of production volume, sales value, and variety of useful derivatives.[1] It is primarily used for the production of such polymeric materials as fabricated plastics, fibers, films, resins, adhesives, and elastomers. Propylene is perhaps the oldest petrochemical feedstocks and is one of the principal light olefins.[2] This olefin is used to produce many end products such as plastics, resins, fibers, etc. It is used widely as an alkylation or polymer gasoline feedstock for octane improvement.[3] In addition, large quantities of propylene are used in plastics as polypropylene, and in chemicals like acrylonitrile, propylene oxide, 2-proponal, and cumene. The major source of ethylene throughout the world is the pyrolysis of hydrocarbons. Propylene is produced primarily as a by-product of petroleum refining and of ethylene production by steam pyrolysis. As conventional petroleum feedstocks become more expensive or scarce as source of ethylene, olefin manufacturers will be forced to look toward unconventional sources.[4]

1.2 Existing Technologies for C-C Coupling

Methane and synthesis gas, which is a mixture of CO and H_2, have been looked upon as the most promising alternative feedstock for the production of longer chain molecules. Much work has been done toward developing methods for direct methane conversion to intermediates as diverse as methanol and formaldehyde.[5-10] These intermediates can be further processed to produce liquid hydrocarbons. The following chart can summarize the conversion methods:

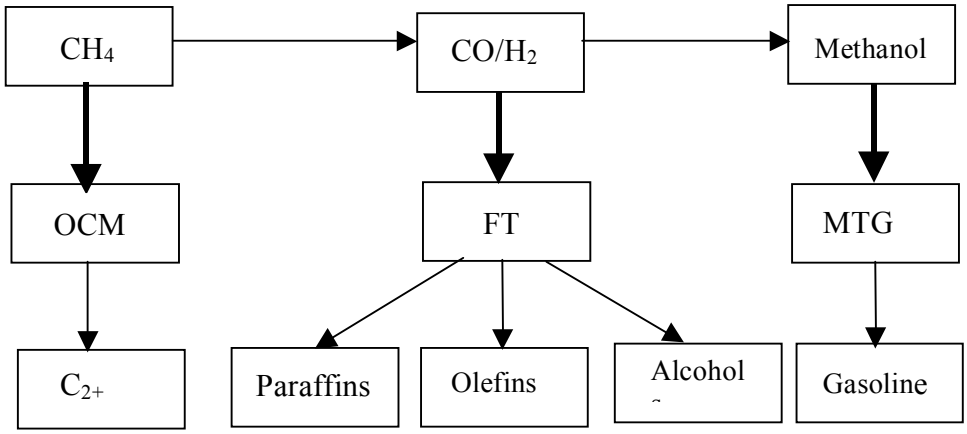

Figure 1.1 Flowchart of longer chain hydrocarbons production technologies from methane; OCM= Oxidative coupling of methane, FT= Fischer-Tropsch synthesis, MTG= methanol to gasoline.

The Fischer-Tropsch synthesis (FTS) is one of the available methods for forming higher molecular weight products from smaller ones.[11-14] This process uses CO and H_2 as feedstock and a suitable catalyst to produce longer chain molecules. Historically Fe and Co are used as FT catalysts but Ni and Ru are also typical FT catalysts capable of producing higher molecular weight hydrocarbons.[15] The products of the FTS are gasoline, diesel fuel, waxes, olefins and

alcohols but the desired product selectivity can be increased by the use of suitable catalyst. The hydrocarbon formation reactions are as follows:

Alkane formation	$(n+1)H_2 + 2nCO \leftrightarrow C_nH_{2n+2} + nCO_2$
	$(2n+1)\ H_2 + nCO \leftrightarrow C_nH_{2n+2} + nH_2O$
Alkene formation	$nH_2 + 2nCO \leftrightarrow C_nH_{2n} + nCO_2$
	$2nH_2 + nCO \leftrightarrow C_nH_{2n} + nH_2O$
Alcohol formation	$2nH_2 + nCO \leftrightarrow C_nH_{2n+1}OH + (n-1)\ H2O$

The FTS is a polymerization reaction with the following steps[16]

1. Reactant adsorption
2. Chain initiation
3. Chain growth
4. Chain termination
5. Product desorption
6. Readsorption and further reaction.

The most important mechanism for the hydrocarbon formation on cobalt, iron and ruthenium catalysts is the surface carbide mechanism by CH_2 insertion.[17] The monomer of the carbide mechanism is a methylene (CH_2) species. CO and H_2 are assumed to adsorb dissociatively. Several species like CH, CH_2, and CH_3 can be formed this way.

Chain growth occurs by the insertion of the monomer in a growing alkyl species. Termination can take place by abstraction of hydrogen to an olefin or addition of a CH_3 species or hydrogen to form paraffin (Figure 1.2). Since the FT synthesis involves a chain growth mechanism, which obeys Anderson-Schultz-Flory kinetics, this poses the problem in designing the process to produce a narrow carbon number range product.[18]

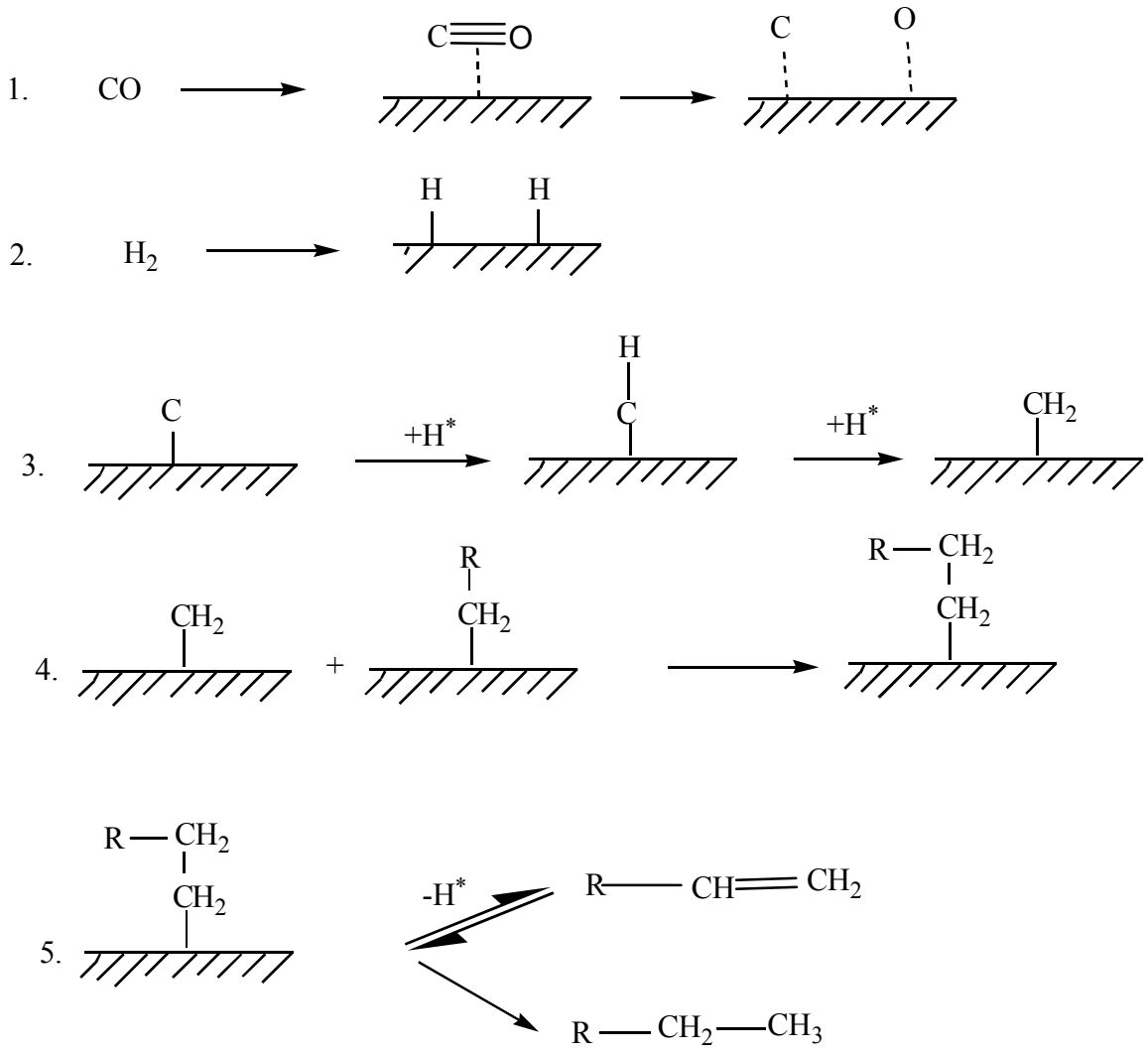

Figure 1.2 Possible mechanism of Fischer-Tropsch chain growth; H^* = surface hydrogen.

Higher molecular weight products can also be formed from methane via methanol. The process is based on selective conversion of methanol using the shape selective zeolite ZSM-5 to yield an aromatic product, which boils in the gasoline range. The methanol is selectively produced from syngas over copper-based catalyst using proven technology. The shape selective zeolites produce hydrocarbon materials from methanol that are predominately in the gasoline range and have both aromatic and aliphatic components. More of the higher-octane gasolines blending stocks are produced by this process than the Fischer-Tropsch process. The shape selective zeolites are intermediate in pore dimension between the familiar wide-pore faujasites and the very narrow-pore zeolite A. It is pore dimension that controls product distribution. A typical product distribution obtained with shape-selective zeolites, expressed as percent weight of the total carbon fraction is: (aliphatic) C_4, 26; C_5, 10; C_{6+}, 4; and (aromatic) benzene, xylenes, trimethylbenzenes, and tetramethylbenzenes, 41.[19]

Oxidative coupling of methane (OCM) is another available technology for the direct conversion routes to form coupling products from methane. In OCM reaction, CH_4 and O_2 react over a catalyst at elevated temperatures to form C_2H_6 as primary product and C_2H_4 as secondary product. The reactions are the following:

$$CH_4 + ¼\ O_2 \leftrightarrow ½\ C_2H_6 + ½\ H_2O$$

$$CH_4 + ½\ O2 \leftrightarrow ½\ C_2H_4 + H2O$$

Unfortunately, both CH_4 and C_2H_4 may be converted to CO_2, and the single pass combined yield of C_2 products is limited to about 25 %.[20] The selectivity toward C_{2+} can be improved by using appropriate catalysts. Over Rb_2WO_4/SiO_2 catalyst 78% C_2H_4 selectivity at a CH_4 conversion of 32 % was achieved.[21] The mechanism of OCM is addressed in detail in the work of different groups.[22-24] Methyl radicals are formed on the surface and coupled in the gas

phase to produce C_2H_6. Ethylene is mainly a secondary product, although a very small amount occurs as an initial product.

1.3 C-C Coupling from Halocarbons

Halocarbons can also be a promising starting material to form C-C coupling products.[25-27] These molecules serve as precursors for producing surface hydrocarbon intermediates.[28-31] Because carbon-halogen bonds (except C-F) are typically weaker than C-H and C-C bonds and because they can be selectively dissociated, these molecules are viable precursors to selected hydrocarbon fragments. Halogenated hydrocarbons or halocarbons are well known environmental pollutants,[32] and understanding the basic coupling chemistry of the halocarbon fragments on solid surfaces will be useful not only for protection and cleanup technologies but also to produce industrially useful olefins. Dichlorodifluoromethane (CF_2Cl_2) is the model single carbon chlorofluorocarbon (CFC) compound. The main idea is to produce surface carbene species from CFC and then combine these carbene species to form coupling products according to the following reactions:

$$CF_2Cl_2 \xrightarrow{-Cl} :CF_2 \xrightarrow{+H} :CH_2 \xrightarrow{coupling} Olefin$$

$$CF_2Cl_2 \xrightarrow{-Cl} :CF_2 \xrightarrow{Coupling} C_2F_4$$

The technology to selectively form coupling products from CF_2Cl_2 is important because it can help in converting all the single carbon Cl containing halocarbon wastes into useful products. Compounds like CCl_4 can be indirectly converted to CF_2Cl_2 by reacting with HF according to the following reactions[33]

$$CCl_4 + HF \rightarrow CCl_3F + HCl \qquad \Delta G = -10 kJ/mol$$
$$CCl_3F + HF \rightarrow CCl_2F_2 + HCl \quad \Delta G = -23 kJ/mol$$

Thus the technology will not only make it possible to convert the existing CFC stocks, it will also help preventing further pollution by converting chlorocarbons into industrially useful products. Another attractive aspect of the technology is that the HF produced in the hydrodehalogenation reaction can be recycled and reused to react with fresh chlorocarbons.

The formation of molecules with one or more C-C bond from halocarbons has been actively researched, but there are only a few reports devoted to C_1 halocarbons as the starting materials.[34-37] The reaction of CF_2Cl_2 and H_2 catalyzed by Pd/C produced C_2 and C_3 hydrocarbons with ~75% selectivity and C_2H_4 as the major coupling product.[34] Tetrafluoroethylene was observed with Pd-Fe/graphite and Pd-Co/graphite catalysts during the CF_2Cl_2 + H_2 reaction at high CFC: H_2 ratios, whereas on Pd/graphite the reaction was unselective toward coupling products.[36] With Pt based catalysts, Pt/C showed negligible selectivity toward coupling products (total selectivity <5%), whereas Pt-Co/C and Pt-Cu/C showed highest selectivity toward C_2-C_3 hydrocarbons (~50 %) and tetrafluoroethylene (~20%), respectively.[35] Mori et al.[37] studied C-C bond formation in the hydrodechlorination of $CHCl_3$ on Pd/SiO_2. Analyzing the C_2-C_7 products produced in the process they concluded that the hydrocarbons were formed via polymerization of surface C_1 species such as methylene groups. In a recent study, Hou and Ching[38] discussed coupling of halocarbon fragments on Cu (111) surface. They observed formation of a difluorocarbene intermediate which coupled to form CF_2=CF_2.

The biggest challenge of forming coupling products from CFCs is to improve the coupling pathways by suppressing other paths of reactions that result in less attractive products. The use of proper catalyst is the way to selective coupling. An appropriately designed catalyst

will lower the barrier for the desired reaction resulting in a much better selectivity. Understanding the basic chemistry and the relation of surface properties with the chemistry will enable us to design the catalyst that is optimum for the reaction of producing coupling products from CFCs. With this in mind the goal of this work has been to advance the basic scientific knowledge of molecular –level events on catalysts for the conversion of CFCs to useful coupling products.

1.4 Scope of the Thesis

The work presented in the thesis concentrates on the development and basic understanding of catalysts for selectively forming coupling products by hydrodehalogenation of dichlorodifluoromethane (CF_2Cl_2). Chapter 2 of the thesis describes the equipment and experimental procedures used in the investigation. The role of the Cu content in the bimetallic PtCu/C catalyst in coupling products formation from CFC in hydrodehalogenation is investigated and the results are reported in the Chapter 3. The Cu content is varied from 0.32% to 2.8 % keeping the Pt content constant (0.5%) in the activated carbon supported bimetallic catalyst. The catalysts are characterized by chemisorption of H_2, chemisorption of CO, chemisorption of O_2 and hydrogen titration of adsorbed oxygen. Transmission electron microscopy (TEM) and high-resolution electron microscopy (HREM) techniques were also used for catalyst characterization. Chapter 4 of this dissertation presents the investigation on different active sites of the PtCu/C bimetallic catalyst in the coupling products formation from CF_2Cl_2. The PtCu/C (0.5%Pt+0.98%Cu) is exposed to water before reaction and the reduced catalyst is used for

kinetic experiments. Kinetics experiments are also performed with CO in the reaction mixture. Chapter 5 presents investigation on Pd bimetallic catalyst supported on carbon for hydrodehalogenative coupling. Group IB (Cu, Ag) and group VIII (Fe, Co) are used as the second metal with Pd. Finally Chapter 6 summarizes the current work and mentions possible works that can be pursued in future.

2.0 EQUIPMENT AND EXPERIMENTAL SETUP

The chlorofluorocarbon conversion work presented in this thesis is based on experimental research. The design of equipment that could accurately and reliably measure the important parameters in the experiments was critical to the results obtained in this investigation. A variety of experimental techniques were used to measure reaction kinetics, catalyst performance, study molecular adsorption and characterize catalysts and support materials. This chapter describes the experimental equipment used for the different techniques and calibration procedures followed. Details of specific experiments performed are presented in individual chapters to describe the experimental procedures relevant to data presented in each chapter.

2.1 Equipment

2.1.1 Reaction System

The kinetics and catalyst performance measurements were carried out at atmospheric pressure in a stainless-steel flow reaction system consisting of a quartz microreactor (10 mm i.d.) equipped with a quartz frit to support the catalyst. A flow diagram for the reaction system is shown in Figure 2.1. The entire system is compactly arranged on a movable cart, which allowed

for easy positioning. The system interfaced with house electric lines to supply power to the various instruments and electronics, with gas tank lines routed from a common tank-holding area and vent lines that were routed from the system to a constant air velocity laboratory exhaust system. The materials used in this study were all gases at room temperature and were drawn from individual gas tanks. For gases such as He, H_2, C_2H_4, and N_2 tanks were equipped with dual stage pressure regulators that reduced typical tank pressures of ~ 2000 psi to line pressures of ~ 100 psi. Dichlorodifluoromethane was contained in tank as liquid and was available at their vapor pressure at room temperature (boiling point –29.8^{o}C, vapor pressure at room temperature 82 psig). The low pressures allowed the use of needle valves at the outlet of these tanks along with a tank pressure gauge. Each gas line was equipped with a check valve, which prevented back-mixing due to pressure fluctuations, a 0.5 or 2 micron filter and at least one ball valve. Gaseous reactants were metered using mass flow controllers (MFC, Brooks Instruments model 5850E) and mixed prior to entering the reactor. An electronic unit regulated the power supply and flow readouts from the MFCs. Prior to entering the reactor a 3-way needle valve controlled the space velocity of the reaction mixture. All lines downstream of the reactor were heated to ~ 50 ^{o}C to minimize the condensation of reactants due to pressure increases. This also minimized the possibility of high molecular weight chlorocarbons formed during the reaction plugging up the tubing.

The reactor was a 4mm i.d. quartz U-tube with a 10 mm i.d. section that contained the porous quartz frit to support the catalyst powder. The reactor was attached to the feed system via two glass-to-metal CAJON fittings and could be removed easily for loading the catalyst samples. The reactor zone containing the catalyst was heated by an electric furnace and the catalyst temperature was measured and controlled with an accuracy of ± 1 K using a temperature

controller (Omega model CN2011). The catalyst temperature was measured by an Omega type K thermocouple placed in a 1mm i.d. quartz sleeve that was in contact with the quartz frit in the reactor. This thermocouple also supplied the "measured variable" to the temperature controller, which operated in a feedback PID loop to control the heat input to the electric furnace surrounding the reactor.

The reactor effluent was analyzed by on-line GC and, when necessary, GC-MS to identify the reaction products. The GC (HP 5890 series II) was equipped with a 15 ft 60/80 Carbopack B/5 % Fluorocol packed column (Supelco) and a flame ionization detector (FID) capable of detecting concentrations > 1 ppm for all CFCs, chlorocarbons and hydrocarbons involved in this study. The on-line HP GC/MS system consisted of a HP 5890 series II plus GC (also equipped with a Fluorocol column) connected to a HP 5972 Mass Selective Detector. Gaseous samples of the reactor effluent were injected in the GC column using an automatic, air-actuated 6-port sampling valve equipped with a 100 μL sample loop. In addition, the GC/MS used a 3-way splitter valve at the GC and MS interface (shown in Figure 2.2) to reduce sample volume entering the MS. This arrangement provided good MS ultimate pressures and adequate sample volume for accurate analysis. For transient kinetics experiments where several samples were collected each minute, an electrically actuated 16-loop sample valve was used. Both, the GC and the GC/MS were interfaced to separate computers running HP Chemstation and MS Chemstation software respectively. All raw data output from GC or GC/MS measurements could be processed using these soft wares and converted to kinetics parameters such as concentration and conversion.

2.2 Instrument Calibration

Calibration of metering devices such as MFCs as well as analytical instruments was performed following manufacturer guidelines. General procedures for calibrating equipment are outlined below along with a few specific examples.

2.2.1 Temperature Controllers

Depending upon the type of thermocouple used and the range of operation, the temperature controllers needed to be calibrated. The controller was calibrated by the manufacturer when assembled. A thermometer placed in the furnace gives the actual temperature, which can be compared to the temperature readout on the controller. Necessary calibration equation between thermocouple readout and thermometer reading can be thus determined. No such equation was required for this research, the discrepancy being within the controller accuracy of +/-1 K.

The PID (proportional, integral and differential) control parameters for the controller were set as explained in the manual. This ensured faster and better control of the temperature and reduced oscillations and overshooting, especially when step change was imposed.

2.2.2 Mass Flow Controllers

A MFC was factory calibrated for specific gas and its calibration became necessary when used for any other gas. Though it was found that the calibrations for the MFCs do not change drastically with time to introduce errors beyond the accuracy of a MFC, it is a good practice to calibrate mass flow controllers at regular intervals of time (whenever a tank is replaced by a new one, a new equipment is connected, tubing is changed or rearranged). Furthermore, it has always been observed that the calibration obtained for MFC had good linearity (correlation factor >99.5%). Even between two calibrations, random checks helped avoid any error in flow. This was done prior to or even during an experiment by switching the flow momentarily through the bubble flow meter and measuring the flow rate.

To calibrate a MFC, the gas is flown through the bypass or through an empty reactor. The idea is to calibrate with the system under conditions as close as possible to those, which will be used in the experiment. Use of an empty reactor will mimic the experimental conditions to some extent. The procedure described below refers to a single gas, but the calibration should be performed independently and individually for all gases following the same procedure. Figure 2.4 shows the typical fits 4 %CO in He flows using a MFC.

The tank regulator delivery pressures were to the following values: 20 psig for CF_2Cl_2, 80 psig for He, 50 psig for H_2 and 50 psig for N_2, which was used as a career gas in the GC. An empty reactor was connected and the gas (whose MFC is to be calibrated) was flown through it and was checked for leaks. The three-way valve placed downstream to appropriate position was switched so that the gas flowed through the bubble flow meter. The soap solution in the bulb of the flow meter was checked to make sure that it was adequate in quantity and wets the flow

meter walls. The MFC reading was set to a certain value (say 5.0) using the knob on the front panel of its control unit. The flow was measured through the bubble flow meter thrice using a stopwatch. The average of the three readings was considered. This procedure was repeated for different MFC settings and the average flow was measured each time. A linear fit (correlation factor of >99.5% is acceptable) should be achieved between the MFC values and corresponding average flows. Care should be taken to calibrate the MFC in the actual range of flows, which would be used in experiments.

2.2.3 GC Calibration

To quantify GC areas, the response of the FID detector must be determined. This involves developing a calibrating function (response factor for FID) between the detector area of a component and its concentration in the stream. The amount of a species entering the GC (and its area) is related to the pressure and volume in the sample loop. The loop volume always remains constant but the pressure varies depending upon the flow rate and other factors such as back pressure.

The carrier gas carrying the reactant and hydrogen were mixed appropriately to achieve desired concentration. Three injections were made each with the gases flowing through the bypass and then through the reactor. The procedure was repeated at the end of the experiment to note and account for the change in the flow. A deviation in the areas of <10% of the average area was deemed acceptable for the current work. The response factor was thus directly determined.

As calibration depends upon the GC settings as well, it is necessary to record several parameters. It is also required to note down the retention times as during the actual experiment the component is identified using its retention time.

2.3 Concerns and Cautions

The following list outlines the essential procedures, which must be performed before, during and/or after conducting an experiment.

Checking the system for leak(s) after new connections. This is possible with the use of a leak detector liquid for atmospheric pressure systems and by using a MS for the vacuum system.

Using conditioned GC and GC/MS columns with timely checks for retention times and response factors.

Using different sets of spatula, reactor, thermocouple-well for different catalysts.

Allowing the instruments to stabilize before taking each reading (at least 5 min between each injection to GC, 1 min with the valve in the "Load" position, about 5 min after changing the flow using a MFC and 1 minute after zeroing pressure gauges).

Material Safety Data Sheets (MSDS) must be obtained for every reactant used and major product being formed during the reaction.

Caution should be maintained while handling hazardous gases such as H_2 and HCl with the use of continuous gas monitoring systems. Explosive and corrosive gases like CF_3COCl should be handled only in hoods with necessary protective equipment.

Vent lines should be checked frequently to ensure leak-free operation and a list of possible effluents from reaction studies should always be maintained.

Safety reviews of equipment and experiments should be made frequently and design improvements to make laboratory operations safer should be an ongoing effort in every graduate student's work.

The GC, GCMS and the reaction system should be maintained properly. The oil in the vacuum pump should be replaced every six months. The filters for the house air should be checked regularly.

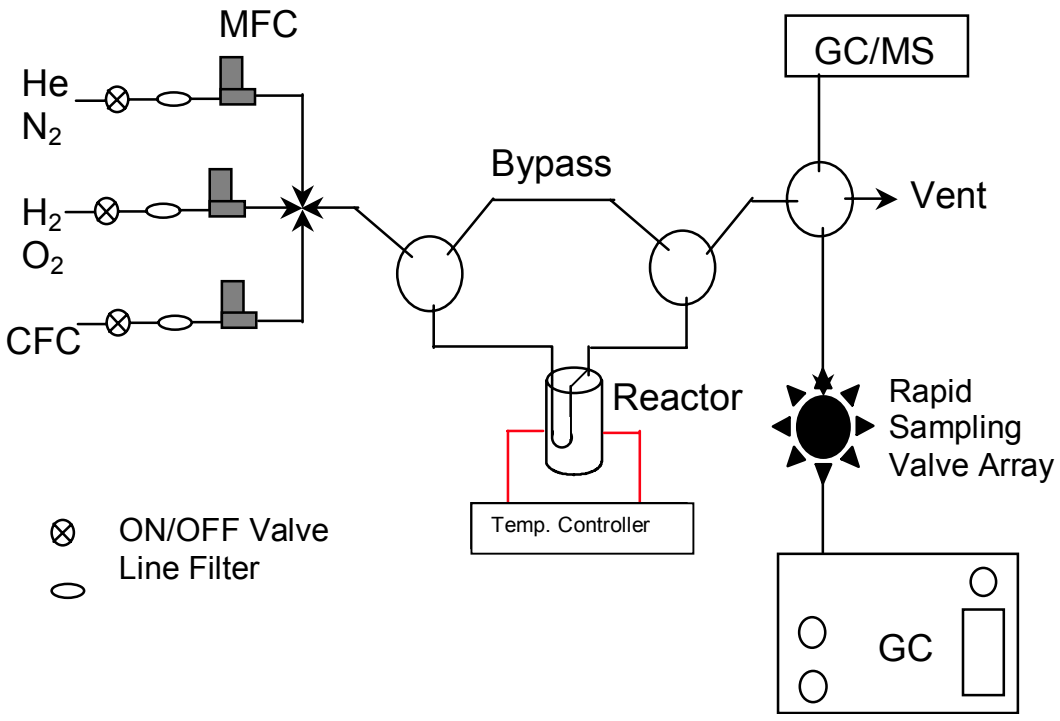

Figure 2.1 Reaction system for CFC kinetics and catalyst performance measurements

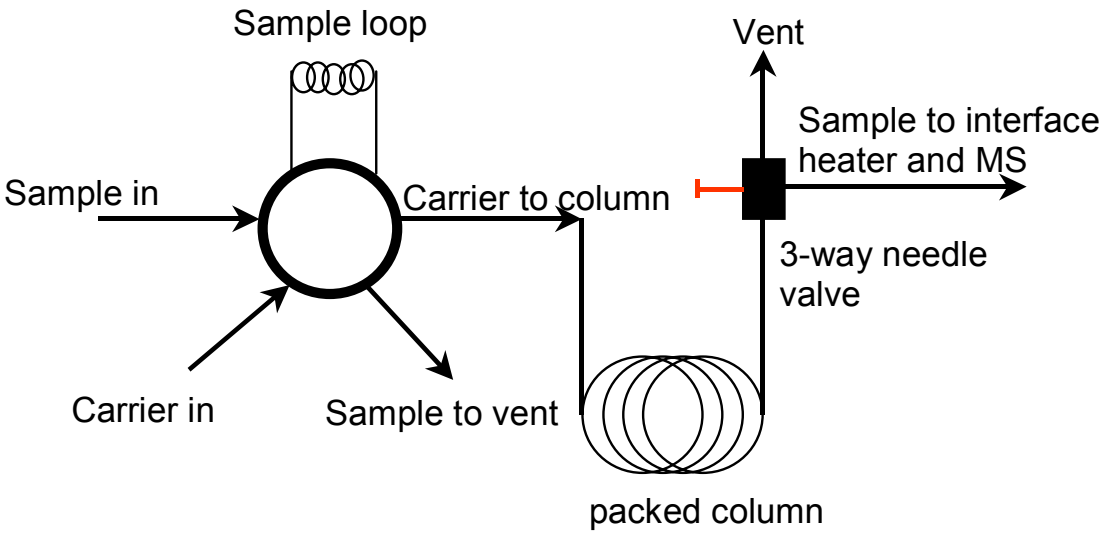

Figure 2.2 Mass spectrometer sample injection flow diagram.

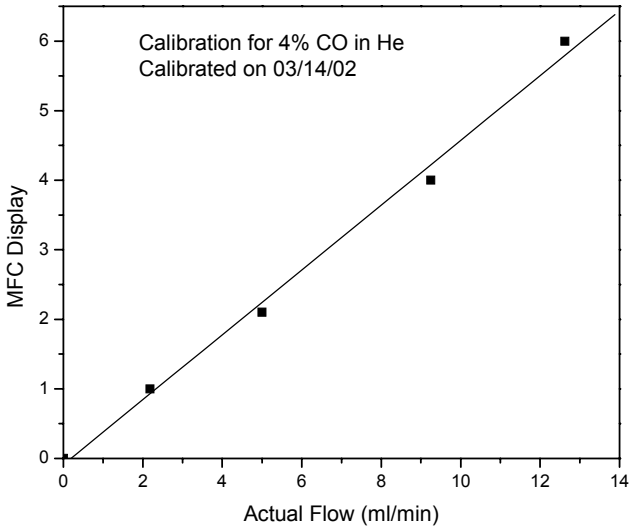

Figure 2.3 Calibration of MFC for 4% CO in He

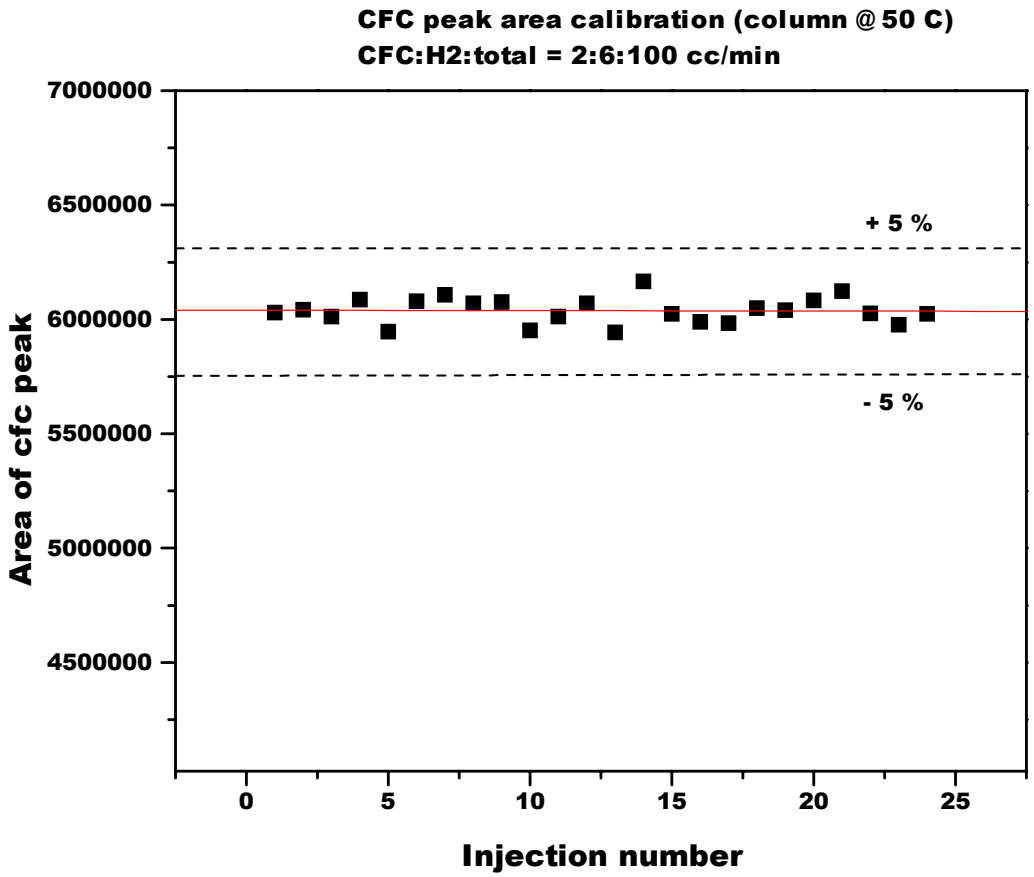

Figure 2.4 GC peak area for CF_2Cl_2 (as a measure of FID response) for 25 sample injections at identical conditions

3.0 EFFECT OF CU CONTENT OF PTCU/C BIMETALLIC CATALYST ON THE REACTION OF HYDROGEN AND DICHLORODIFLUOROMETHANE: FORMATION OF HIGHER MOLECULAR WEIGHT COUPLING PRODUCTS

3.1 Introduction

Chlorofluorocarbons (CFCs) have had a lasting effect on the environment. CFCs are the major sources of stratospheric chlorine, which is responsible for the depletion of the ozone layer.[1] While many western countries have stopped the production of CFCs, over 120400 metric tons of CFCs were produced worldwide in the year 2000.[2] Thus technology to convert CFCs into environmentally benign and industrially useful products is still required. Catalytic hydrodechlorination is one of the available technologies and in addition to the environmental advantages, it has obvious economic merits because the resulting products can be recovered and recycled for use.[3] Studies of the hydrodechlorination of CFCs have been mainly focused on the full or partial removal of Cl atoms from the molecules to obtain alkanes or partially halogenated alkenes.[4-6] However, the production of higher molecular weight coupling products through the hydrodehalogenation of CFCs may also be possible.[7-9]

The formation of molecules with one or more C-C bonds from halocarbons has been actively researched, but there are only a few reports devoted to C_1 halocarbons as the starting materials.[10-12] The hydrodechlorination of CF_2Cl_2 catalyzed by Pd/C produced C_2 and C_3 hydrocarbons with ~75% selectivity and C_2H_4 as the major coupling product.[10] Tetrafluoroethylene was observed with Pd-Fe/graphite and Pd-Co/graphite catalysts during the CF_2Cl_2 + H_2 reaction at high CFC:H_2 ratios, whereas Pd/graphite was unselective toward coupling products.[12] With Pt based catalysts, Pt/C showed negligible selectivity toward coupling products (total selectivity <5%), whereas Pt-Co/C and Pt-Cu/C showed the highest selectivity toward C_2-C_3 hydrocarbons (~50%) and tetrafluoroethylene (~20%), respectively.

Though it has long been known that alloying significantly changes the catalytic properties,[13-15] it is still a matter of debate whether this change is due to ensemble effects,[16-17] structure effects,[18] or electronic effects.[19] In many cases the alloy surface composition and structure are different from the bulk and this composition and the surface structure depends heavily on the reactants and reaction conditions.[20] Thus using bimetallic catalysts creates the opportunity to tune the catalyst properties to achieve the desired results. In a previous investigation,[21] Pt-Cu/C was shown to be highly selective toward coupling products in the reaction of CF_2Cl_2 and H_2. The present investigation centers on the role of Cu content in controlling the chemistry catalyzed by bimetallics. The Cu content was varied keeping the Pt content constant in the activated carbon supported bimetallic catalyst to investigate the role of Cu as well as the Pt to Cu atomic ratios in the formation of coupling products in the hydrodehalogenation of CFC.

3.2 Experimental

3.2.1 Catalyst Preparation and Characterization

Activated carbon (BPL F3, 6x16 mesh, Calgon Carbon) was crushed and sieved to obtain a fraction of 24-60 mesh (1400 m^2/g surface area; 2.4 nm average pore diameter) to use as a support. The 24-60 mesh fraction was then co-impregnated with an aqueous solution of $H_2PtCl_6.6H_2O$ (Alfa, 99.9%) and $CuCl_2.2H_2O$ (MCB Manufacturing Chemists, 99%). The material was allowed to equilibrate overnight before drying at ambient temperature and pressure for 24 h. It was then dried at 100 ^{0}C for 2 h in vacuum (~25 Torr). The catalyst nomenclature is defined according to the Pt to Cu molar ratio. For example, a catalyst with Pt to Cu ratio 1:6 is referred to as Pt1Cu6. The compositions of all the catalysts are listed in Table 3.1.

Chemisorption and BET measurements were carried out using a volumetric sorption analyzer ASAP 2010 and ASAP 2010 Chemi (Micromeritics ®). The metal-adsorbate ratio was determined from the irreversibly adsorbed CO, H_2 or O_2. The adsorbate – metal stoichiometry was assumed to be equal to 1 for CO and 2 for both H_2 and O_2. For each catalyst CO, H_2, O_2 chemisorption and titration of adsorbed oxygen with H_2 (HT) were performed sequentially with the same sample at 35 ^{0}C. Prior to measurement, the catalyst was reduced at 300^{0}C for 1 h in flowing H_2 (Praxair, 99.999%). The reduction was followed by evacuation for 1.5 h at 350 ^{0}C. Then the catalyst was cooled, the CO chemisorption was performed and the catalyst was reduced at 350 ^{0}C for 1 h and evacuated for 1.5 h at the same temperature. Next, H_2 chemisorption was conducted after which the catalyst was again evacuated at 350 ^{0}C for 1.5 h. This was followed

by O_2 chemisorption, evacuation at 350 ^{0}C for 1 h and H_2 titration. The dispersion results are shown in Table 3.1.

3.2.2 Catalytic Experiments

The hydrodechlorination of CF_2Cl_2 (Atochem, >99%; detectable impurities: CHF_2Cl ~0.25% and CH_3CF_3 ~0.25%) was conducted at atmospheric pressure in a stainless steel flow reaction system consisting of a down-flow quartz micro reactor (10 mm i.d.) equipped with a quartz frit to support the catalyst. An electric furnace was used to heat the reactor zone containing the catalyst. The catalyst bed temperature was measured and controlled with an accuracy of ± 1 ^{0}C (Omega model CN2011). The gas flows (CFC, H_2, Praxair, 99.9%; He, Praxair, 99.9%) were metered with mass flow controllers (Brooks Instruments, model 5850E) and mixed prior to entering the reactor. The reactor effluent was analyzed by on-line GC and by GC/MS to identify the reaction products. The GC (HP 5890 series II) was equipped with a 15 ft 60/80 Carbopack B/5% Fluorocol packed column (Supelco) and a flame ionization detector (FID) capable of detecting concentrations >1 ppm for all CFCs, chlorocarbons and hydrocarbons under investigation. The on-line HP GC/MS system consisted of a HP 5890 series II Plus GC equipped with a Fluorocol column connected to a HP 5972 Mass Selective Detector. A 16-loop sample valve (VICI) was attached to the GC to collect sample without waiting for the GC analysis to finish. The valve was used to collect samples during the very early stages of the reaction.

Prior to reaction, the catalyst was treated with a mixture of H_2 (20 ml/min) and He (30 ml/min) as it was heated from 27 ^{0}C to 400 ^{0}C at the rate of 5 ^{0}C /min and then held at 400 ^{0}C for 120 min. The catalyst was cooled in flowing He (30 ml/min) to the reaction temperature, 250 ^{0}C, and the reactant mixture was introduced. The reaction was conducted at the CF_2Cl_2 to H_2 molar ratio of 1 (2 ml/min of each) with He (26 ml/min) as diluent. The CF_2Cl_2 to H_2 molar ratio used in this work is the stoichiometric ratio required for the dechlorinative dimerization of CF_2Cl_2 to C_2F_4. In all cases the conversion was kept below 5% to maintain condition appropriate for the differential reactor assumption. All experiments were stopped after the conversion had reached to < 0.2 %.

For all experiments the total flow rate was 30 ml/min (balance by pure He flow) and the catalyst weight was ~0.03 g. The selectivities (S_i) toward detectable carbon-containing products were calculated as follows:

$$S_i = \frac{n_i C_i}{\sum_i n_i C_i},$$

where n_i and C_i are the number of carbon atoms in a molecule and the mole concentration of the product i in effluent gas, respectively. The formation of HCl was detected by GC/MS but not quantified.

The reaction rates per gram of catalyst was calculated by applying the differential reactor approximation in the form

$$\text{Rate (mmol/gsec)} = F*y/W,$$

where F is total molar flow rate, y is the mole fraction of reactant converted, and W is the catalyst weight. The turnover frequencies (TOF) were calculated using the expression

$$\text{TOF } (s^{-1}) = R*MW_{Pt} / M*d,$$

where R is the rate per gram of catalyst, MW_{Pt} is the molecular weight of Pt, M is the Pt loading percent, and d is dispersion.

3.2.3 **TEM Experiments**

Transmission electron microscopy (TEM) studies were conducted using a JEM2010 (JEOL) electron microscope with a resolution of 0.14 nm and an accelerating voltage of 200 kV capable of distinguishing metal particles as small as 10 Å on the support surface. Reduced and used catalysts were generated from the kinetics system described above and were placed in tightly sealed glass vials for transport to the microscopy system. Sample preparation consisted of hand grinding under ethanol for 20 to 60 sec followed by further dispersion with ultrasound at 35 kHZ. Drops of suspension were then placed on gold grids for examination. Digital Fourier-analysis (FFT) was used to analyze the HREM images. The mean diameter of all particles observed, d_m, and surface weighed average particle size, d_{ss}, were calculated by using the following formulas:

$$d_m = \frac{\sum_1^N d_i}{N},$$

and

$$d_{ss} = \frac{\sum_1^N d_i^3}{\sum_1^N d_i^2},$$

where d_i is particle diameter and N is the total number of particles.

3.3 Results

3.3.1 Catalyst Characterization

The results of chemisorption measurements of the carbon supported Pt, the bimetallic Pt-Cu catalysts and the pure support are shown in **Table 3.1**. The CO/Pt ratios are in the range of 43.6-49.1 for all PtCu bimetallics and for monometallic Pt catalyst the ratio was 26.5. It is important to remember that the CO chemisorption stoichiometry is unknown because the proportion of chemisorbed species in the linear and bridged forms can vary. Furthermore, the adsorption properties may also depend on the metal particle size.(22) The H/Pt ratios for all the catalysts are in the range of 3-5, which is significantly lower than that of CO/Pt. Lower hydrogen uptakes, compared with those of CO, were also observed for bimetallic Pt-Sn.(23) Platinum, Cu and the support chemisorbed oxygen irreversibly (**Table 3.1**). The uptake of oxygen increased while the ratio of O/(Pt+Cu)t decreased with increasing Cu loading . For Pt/C the ratio was 70.5 and for PtCu/C bimetallics the ratio ranged from 70.5 to 12.1 (**Table 3.1**).

The chemistry of hydrogen titration follows the reaction $O_{(s)}+3/2H_2 \rightarrow H + H_2O$.[22] The results of hydrogen titration (Table 3.1) do not correlate with those of CO chemisorption; H/Pt_t(HT) ratio decreased with increasing Cu/Pt atomic ratio. It is important to note that Cu is incapable of reducing adsorbed oxygen at 35 ^{0}C.

Although each metal dispersion measurement method has drawbacks, one can obtain a good qualitative understanding by performing a combination of techniques. For example, from the $O/(Pt+Cu)_t$ ratios (Table 3.1) it is clear that the mean size of the bimetallic particles

increased as the metal loading increased, while the fraction of Pt atoms exposed remained essentially the same (from constant H uptake, Table 3.1) as Pt diluted Cu.

The carbon support consisted of distorted graphite layers, which formed fullerene like microstructures (

Figure 3.1). The diameters of the carbon spheres formed in this case were approximately 50 Å. In some places multilayer piles (2-5 layers) characteristic of graphite with the interlayer distance of approximately 3.5 Å were observed. The particles of the Pt in monometallic Pt/C catalyst were evenly distributed on the surface (Figure 3.2a) with a diameter in the range of ~15 to ~40 Å (Figure 3.2b). The average particle size of the metal particles, dm and surface weighed average particle size dss were 25 and 30 Å, respectively. The TEM micrographs of PtCu/C catalysts after reduction showed the existence of metal particles in the range of 13-30 Å in size and also quasi-spherical particles (Figure 3.3 and Figure 3.4). Phase of copper oxide was identified in the quasi-spherical particles by electron microdifraction and HREM images. The CuO is most likely the result of exposing the reduced catalyst in air before the TEM studies. As the Cu content in the Pt-Cu catalyst was increased, the size of the copper oxide particles also

increased. For example, the size range was 200-500 Å for Pt1Cu9 while for Pt1Cu18 the size was as large as 5000 Å. However, the morphology of the CuO particles was the same for all the Pt-Cu bimetallic samples. Dot scattering centers were observed for the reduced bimetallic catalysts (Figure 3.5). Tentatively these were attributed to the presence of isolated or aggregated copper ions on the carbon support.

3.3.2 Kinetics

All PtCu bimetallic catalysts supported on activated carbon BPLF-3 hydrodechlorinated CF2Cl2. For all catalysts, the conversion with time on stream (TOS) initially increased to maximum after ~5 h and after that a continuous deactivation of the catalysts was observed (**Figure 3.6**). The highest conversion for the catalysts ranged from 3.8-2.2 %. After approximately 65 h of TOS the activity of Pt1Cu2 decreased by ~40%, Pt1Cu6 decreased by ~96%, Pt1Cu9 decreased by ~38%, and Pt1Cu18 decreased by 34% from their respective highest activities.

The average selectivity distribution toward C_1 and coupling products after 5 min of TOS was clearly a function of Cu content in the catalysts (Figure7). The total C_1 selectivity decreased from 88% for Pt1Cu2 to 70% for Pt1Cu18. All catalysts produced CH_4 as the major C_1 product with a selectivity of ~70%- ~55% as well as CHF_2Cl with 10-15 % selectivity during the initial 5 min of TOS. Difluoromethane (CH_2F_2) was observed with <10 % only on Pt1Cu2/C and Pt1Cu6/C. The total coupling selectivity ranged from 10% for Pt1Cu2 to 35% for Pt1Cu18. The monometallic Pt /C produced coupling products with <5% selectivity,[10] whereas ~35% initial

selectivity toward hydrocarbon coupling products was observed for the Pt1Cu18 /C catalyst. Ethylene was the major coupling product on the Pt-Cu bimetallic catalysts during the initial TOS and the ethylene selectivity increased with increasing Cu content in the catalysts. Ethane was formed on both the Pt/C[10] and the Pt-Cu/C bimetallic catalysts with ~3% selectivity. The C_3 (C_3H_6) products were observed only with the Pt1Cu18/C catalyst. No fluorinated-coupling product was observed for any of the catalysts during the initial 5 min TOS.

The selectivity pattern of the C_1 reaction products changed with TOS (Figure 3.8). The selectivity toward CH_4 for all the catalysts continuously declined with TOS. The CH_4 selectivity decreased from 62% to50% for Pt1Cu2, from 50% to 35% for Pt1Cu6, from 70% to 25% for Pt1Cu9, and from 58% to 25% for Pt1Cu18 after 65 h TOS. Difluoromethane selectivity was about 5% for Pt1Cu2 for the entire length of the experiment. On Pt1Cu6 the CH_2F_2 selectivity was initially 5% and became 0 during 10 h of TOS. The CH_2F_2 selectivity was 2% for Pt1Cu9 and Pt1Cu18 for all along the TOS. Trifluoromethane (CHF_3) was produced only for Pt1Cu6. The production of CHF_3 was detected after 12 h of TOS and the selectivity was 20%; increased gradually to 35% after 65 h of TOS. The selectivity trend for CHF_2Cl varied with type of catalyst. It decreased from 15%- 8% for Pt1Cu2, 12%- 20% for Pt1Cu6, and ~2% for Pt1Cu9 and from ~2 - ~5% for Pt1Cu18 for the entire TOS.

The selectivity toward coupling products also changed with TOS (Figure 3.9). The C_2H_4 selectivity remained almost unchanged at ~8% for Pt1Cu2 whereas the selectivity increased from 3 to 15% toward C_3H_6, and from 1.8 to11.6% for C_4+. The C_2H_4 selectivity increased from 16 to 28% after 10 h of TOS and then decreased gradually to 5%, the C_3 selectivity increased from 20 to 25% within first 5 h of TOS and then decreased gradually to 0 after 60 h of TOS, and C_4+ selectivity increased from 2 to 6% during 5 h TOS and the gradually decreased to 0 within 30 h

of TOS for Pt1Cu6. The production of C_2F_4 started after 20 h of TOS and the selectivity went to a maximum of 15% at around 60 h of TOS and then decreased to 10% after approximately 68 h. The C_2H_4 selectivity increased from 13 to 29mol %, the C_3 selectivity increased from 3 to 25%, and the C_4+ selectivity increased from 1 to 13% during 65 h TOS for Pt1Cu9. The C_2H_4 selectivity increased from 24 to 30%, the C_3 selectivity increased from 5 to 26%, and the C_4+ selectivity increased from 1 to 12% during 65 h of TOS for Pt1Cu18. The C_2H_6 selectivity for all the catalysts was <5%.

3.4 Discussion

The addition of Cu to Pt has a significant effect on morphology and surface characteristics of the particles. Considering the large surface area of the carbon support and low metal loading (<3%), it can be speculated that the metal precursors will be highly dispersed on the support surface. Due to the specific adsorption on the supporting surface, one or both of the components might be strongly anchored to the surface, the mixing of the constituent should, therefore, be achieved either during calcinations or reduction. For the PtCu bimetallic catalyst alloy formation can be thought of by the 'catalyzed reduction model'[24] where Pt particles are formed first because of the easy reducibility, and then mobile Cu^{2+} ions are adsorbed by these Pt particles and swiftly reduced. The very high surface mobility of Pt in presence of H_2[25] may also be helpful for the process. The resulting "cherry" type bimetallic particles consist of a Pt core and a copper mantle. Obviously one cannot expect that all particles on the surface will be bimetallic; formation of monometallic Pt and Cu and Cu rich and Pt rich bimetallic particles are

more practical from the statistical point of view. Above 227 ^{0}C the Pt atoms diffuse into bulk Cu and disordered Pt-Cu surface alloys are formed.[26] Both the reduction and reaction temperatures (400 ^{0}C and 250 ^{0}C respectively) are higher than 227 ^{0}C. So, all these conditions support the possibility of formation of Pt-Cu surface alloy where small Pt islands (may be single atoms) will be surrounded by large number of Cu atoms as the Pt atoms in the Cu enriched surface are not clustered.[27] The kinetics results of the present investigation allow one to ask the question of how do the changes in surface characteristics affect the activity and selectivity of the bimetallic catalysts.

Although Pt shows very negligible selectivity towards coupling, addition of Cu to Pt dramatically increases the coupling selectivity.[11] The coupling selectivity increases monotonically with the increasing Cu content (Figure 3.9) in the catalysts. However, the activity of the catalysts follows the opposite trend with increasing Cu content (Figure 3.6). Dispersion results (Table 3.1) show that the number of exposed Pt atoms increased with addition of Cu. Because of the decreasing activity and lower selectivity toward CH_4 and CH_2F_2, which are the main products on Pt/C,[11] with increasing Cu content, it is reasonable to suggest that the reaction is structure sensitive.[28-30] Addition of Cu may decrease Pt ensembles to sizes that are not big enough for hydrodehalogenation.

Addition of Cu to Pt will not only decrease Pt ensemble size but may also act as an active site. Though the roles of different active sites of Pt-Cu bimetallic particles are not clear in hydrodechlorination, it is well known that Pt has much larger activities with respect to hydrogenation reaction than Cu,[31] which has excellent coupling[32] properties. However Cu cannot readily dissociate H_2 because of the highly activated nature of the process on Cu. This is the reason why Cu alone is inactive; CuCl formed covers the surface and deactivates it; the CuCl

surface cannot adsorb hydrogen but Pt can supply hydrogen atoms for its reduction to Cu. The Pt particles present in the catalyst are responsible for producing CH_4 and other C_1 products and H atoms by dissociation of H_2, which is spilled over to the Cu particles. Works examining the adsorption of H_2 on Ru (001) and Re (001) surfaces precovered with submonolayer coverages of Cu and an ordered Cu_3Pt (111) surface consists of 2 x 2 lattice of isolated Pt atoms completely surrounded by Cu atoms (d_{Pt-Pt} =5.2 A) show a "spillover" of hydrogen atoms, H_a, from the transition metals to noble metal.[33] The electronic effect of alloying should also be considered here.

Considering the model of the catalyst surface one can assume the elementary reaction steps of the reaction. Although there is no clear understanding of the elementary reaction steps during hydrodechlorination reaction, it is widely accepted that $*CF_2$ is the most reactive surface species during the reaction.[34] The selectivity would be determined by the associative desorption of the species helped by hydrogen and the removal of fluorine by adsorbed hydrogen, yielding $*CH_2$, which on Cu surfaces will couple to from C_2H_4 or other higher olefins. In the absence of hydrogen, Hou and Chiang have detected CF_2=CD_2 when both CF_2 and CD_2 are present on Cu (111) surface.[35] The fact that no CF_2=CH_2 is detected can be related to the very transient nature of the $*CF_2$.[36] In presence of H, $*CF_2$ is instantly converted to $*CH_2$. That C_2F_4 has also not been detected for all catalysts except Pt1Cu6 also supports this conclusion. The case of Pt1Cu6 will be discussed in the later part of the discussion. The TEM images showed that the Cu particle size grows bigger with increase in Cu content. This is further supported by the chemisorption results (Table 3.1). The Pt/CO ratios remained relatively unaffected but the O to $(Pt+Cu)_t$ ratios decreased with increase in Cu. On bigger Cu particles, the carbene species formed by the dissociation of C-halogen bonds of the CFC will have a greater chance of finding another

carbene specie to form a coupling product. Also it can be expected that the number of bimetallic particles will increase with increase in Cu content in the catalyst. This phenomenon can also be responsible for a higher coupling selectivity with increasing Cu content.

A very significant change in selectivity pattern is observed from its initial state. For example, for Pt1Cu18 the initial coupling selectivity is ~35 % whereas it increases to ~60% with TOS. This can be explained by speculating that at the very initial stage Pt sites are more active than Cu sites. It has been shown that the presence of Cl on Rh/SiO_2 decreases the hydrogenation activity of rhodium.[37] Thompson et al. have shown that HCl has an inverse first order effect on the rate of hydrodechlorination of CFCs on Pd/C catalyst.[38] If the same effect can be considered for Pt, as the hydrodehalogenation reaction proceeds, the HCl concentration is increased resulting in a decrease in activity of Pt sites. It is interesting to note the relation between the deactivation rates with initial C_1 selectivity of the catalyst. Catalysts with higher initial C_1 selectivity deactivates at higher rates. Deactivation during hydrodechlorination on Pt/C catalyst has been related to the formation of chlorine containing carbonaceous deposits on the metal.[39] As Cu does not form bulk carbide,[32] deactivation of Cu sites by carbonaceous deposits is possibly unlikely. So with TOS the activity of Pt sites decreases, but for Cu sites it remains unchanged because of the facile nature of the halogen removal from the surface by hydrogen. The deactivation process, thus can be related mainly to the loss of Pt active sites and therefore decrease in C_1 selectivity.

The catalytic behavior of Pt1Cu6 demands special attention. It is the only catalyst tested for this contribution, which produces CHF_3 and C_2F_4 in the CFC hydrodehalogenation reaction. This catalyst also deactivates more rapidly than other catalysts (Figure 3.6). Coq et al. have related the formation of C_2F_4 on PdFe/graphite and PdCo/graphite from the hydrodechlorination

of CF_2Cl_2 to the higher concentration of $*CF_2$ surface intermediates.[12] The relatively higher selectivity toward CHF_2Cl on Pt1Cu6 is an indication toward Cl deposition on the surface. Wiersma et al. has also attributed higher CHF_2Cl concentration on the higher surface Cl concentration.[40] The formation of CHF_3 can be considered as a chlorine/fluorine exchange reaction for which a reaction with adsorbed fluorine has to take place. So, the formation of CHF_3 is an indication of the influence of fluorine presence on the metal surface. Therefore, all the above phenomena i.e. higher rate of deactivation, higher selectivity toward CHF_2Cl and CHF3 indicates that the surface halogen removal for Pt1Cu6 is not as facile as the other catalysts. This can be due to lack of H supply on the Cu surface which prevents further reduction of $*CF_2$ to $*CH_2$ and also the removal of surface halogens. As a result of this, the surface becomes poisoned quickly. In this regard one interesting point to note in Figure 3.9b is that the increase of the selectivity toward C_2F_4 is accompanied by a simultaneous decrease in the selectivity toward C_2 and C_3 hydrocarbon. However, it is a matter of future research why this phenomenon occurs only Pt1Cu6/C catalyst.

3.5 Conclusion

The kinetics results of the reaction of CF_2Cl_2 and H_2 catalyzed by PtCu/C catalysts, showed the effect of Cu content on the selectivity pattern. The observation was that the coupling selectivity increased with the increasing Cu content. The Pt/C catalyst showed less than 5% selectivity toward coupling, whereas ~35% initial selectivity toward hydrocarbon coupling products was observed for Pt1Cu18 (0.5% Pt +2.8% Cu) catalyst. The selectivity pattern changed with TOS. All the catalysts showed an increase in coupling selectivity with TOS. This phenomenon suggests that the modification of the catalytic sites is occurring as the reaction proceeds. It was speculated that the alloy formation was by the 'catalyzed reduction model' where Pt particles were formed first because of the easy reducibility, and then mobile Cu^{2+} ions were adsorbed by these Pt particles and swiftly reduced. The resulting "cherry" type bimetallic particles consisted of a Pt core and a copper mantle. The TEM micrographs of PtCu/C catalysts after reduction showed the existence of metal particles in the range of 13-30 Å in size and also quasi-spherical particles. Phase of copper oxide was identified in the quasi-spherical particles by electron microdifraction and HREM images. The CuO is most likely the result of exposing the reduced catalyst in air before the TEM studies. As the Cu content in the Pt-Cu catalyst was increased, the size of the copper oxide particles also increased. For example, the size range was 200-500 Å for Pt1Cu9 while for Pt1Cu18 the size was as large as 5000 Å. However, the morphology of the CuO particles was the same for all the Pt-Cu bimetallic samples. This implies

that the bimetallic particle formation is not complete after reduction and there are scopes to improve alloy formation by better mixing of the precursors.

Table 3.1. Irreversible Gas Uptakes and Apparent Dispersion of PtCu/C Catalysts

Catalyst composition (wt%)	Pt/Cu (at. ratio)	Uptake (μmol/g_{cat}) CO	H_2	O_2	H_2 (HT)	Apparent dispersion (%) CO/ Pt_t	H/Pt_t	O/ $(Pt+Cu)_t$	H/Pt_t (HT)
Support	-	0	0	3.0	0	-	-	-	-
0.49% Pt	∞	6.8	0.2	9.0	8.5	26.5	1.7	70.5	66.4
0.49%Pt+ 0.32% Cu	1:2	10.9	0.5	23.6	4.7	43.6	3.9	62.6	37.8
0.48%Pt+ 0.95% Cu	1:6	11.0	0.4	23.3	1.9	44.8	3.0	26.8	15.4
0.47%Pt+ 1.40%Cu	1:9	12.1	0.6	26.5	0.9	49.1	5.0	21.7	7.2
0.46%Pt+ 2.8%Cu	1:18	10.7	0.4	28.1	0.7	45.2	3.6	12.1	5.9

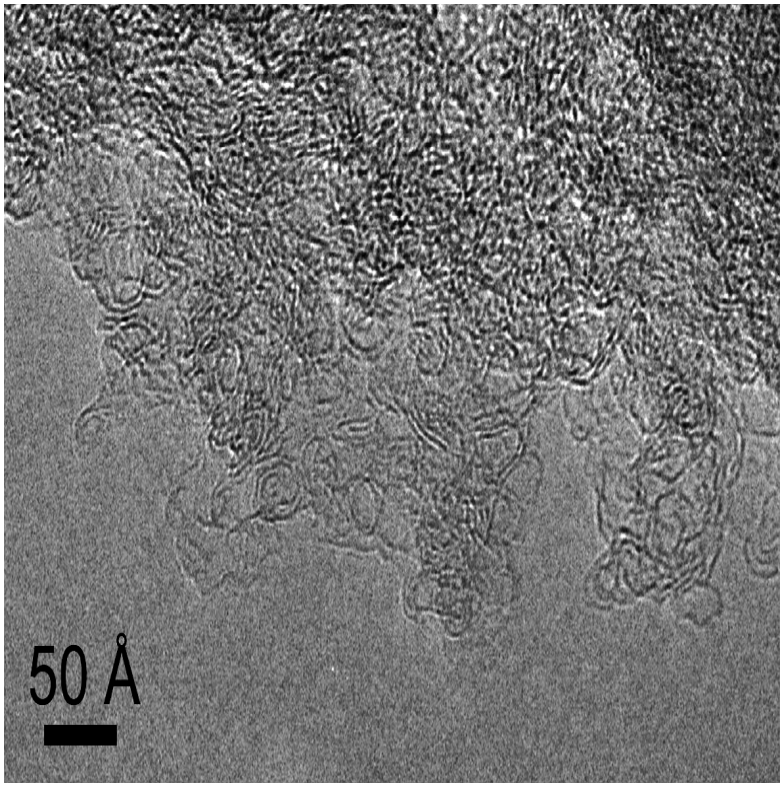

Figure 3.1 HREM image of the BPLF-3 carbon support

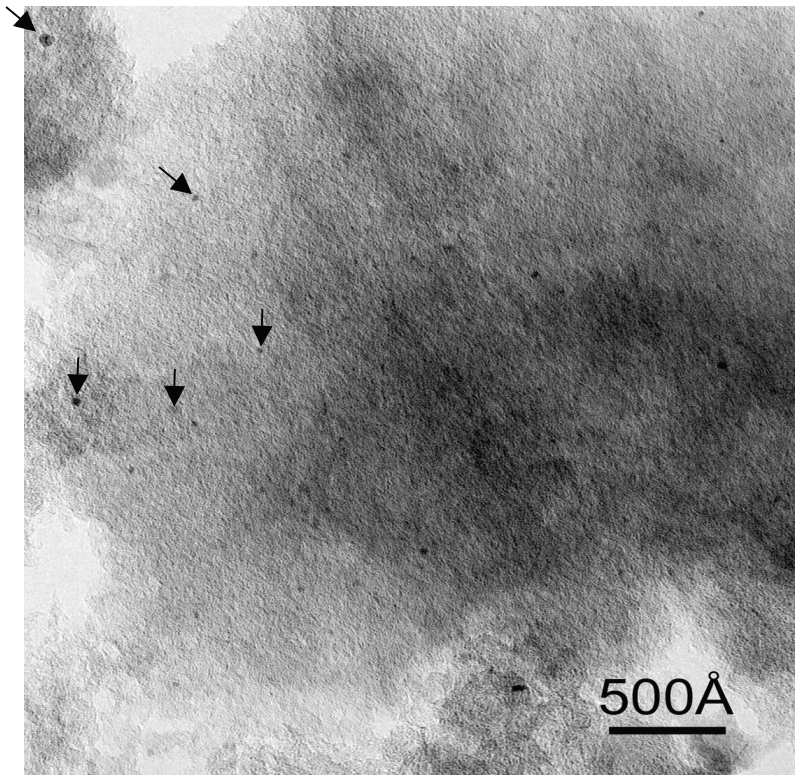

a

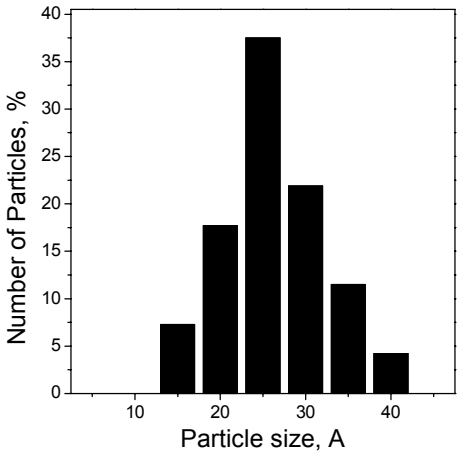

b

Figure 3.2 Pt particles on C support for reduced 0.5 % Pt/C (a); and histogram showing the particle size distribution for reduced 0.5 % Pt/C (b); reduction condition: 400 ^{0}C, in 20 ml H_2 + 30 ml He flow.

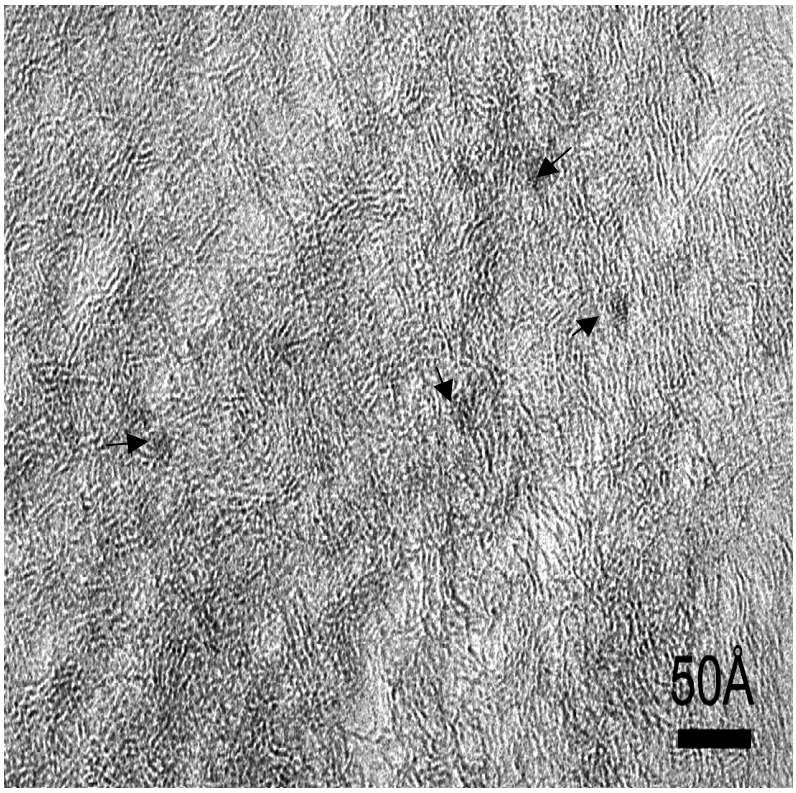

Figure 3.3. Particles on the carbon support of reduced Pt1Cu6/C reduction condition: 400 ^{0}C, in 20 ml H_2 + 30 ml He flow.

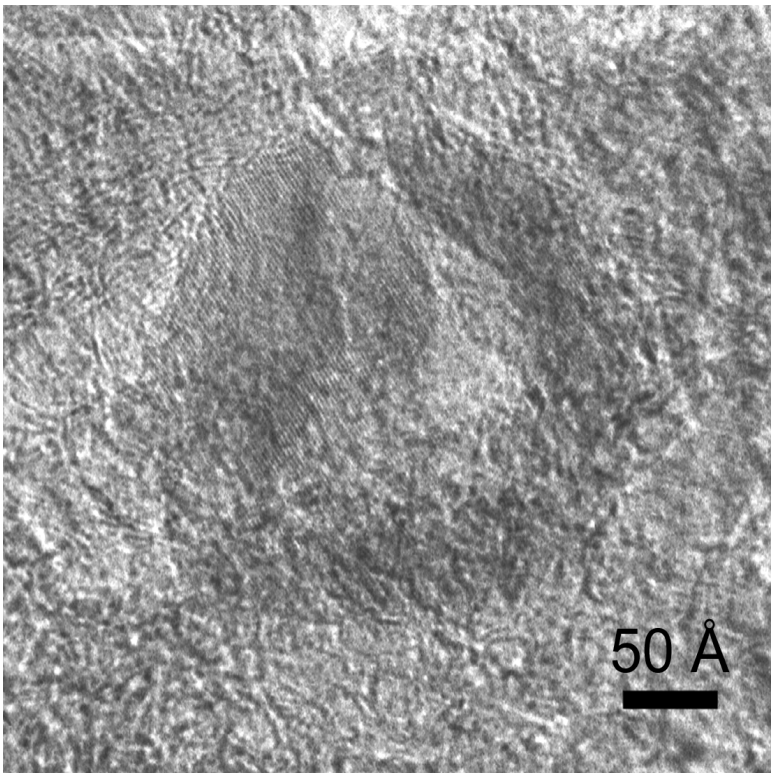

Figure 3.4 CuO particle on carbon support of reduced Pt1Cu9 catalyst ; reduction condition: 400 ^{0}C, in 20 ml H_2 + 30 ml He flow.

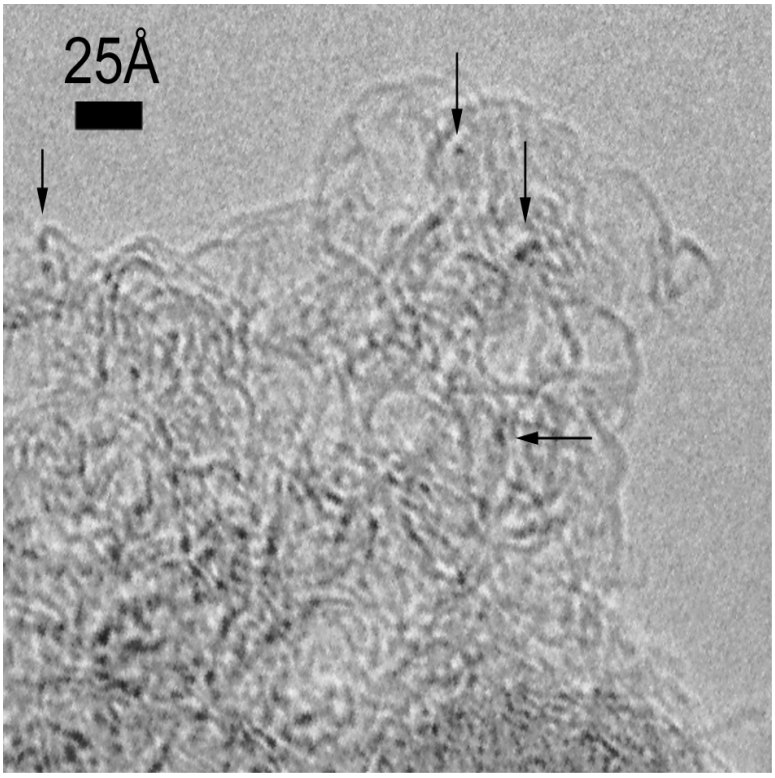

Figure 3.5 Dot scattering centers of reduced Pt1Cu2/C catalyst showing the presence of copper ions; reduction condition: 400 ^{0}C, in 20 ml H_2 + 30 ml He flow.

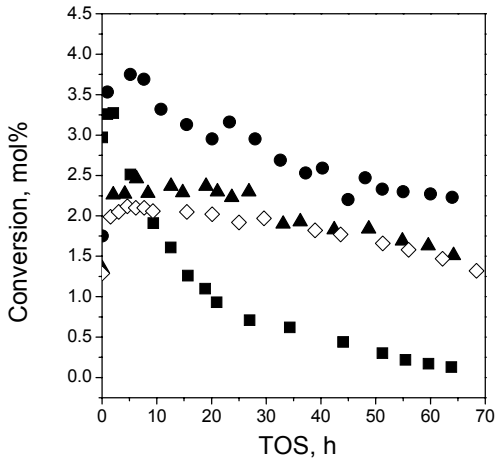

Figure 3.6.. TOS profile of CF_2Cl_2 conversion catalyzed by Pt1Cu2 (●), Pt1Cu6 (■), Pt1Cu9 (▲), and Pt1Cu18 (◊) (250 ^{0}C, 1 atms, CF2Cl2:H_2=1:1).

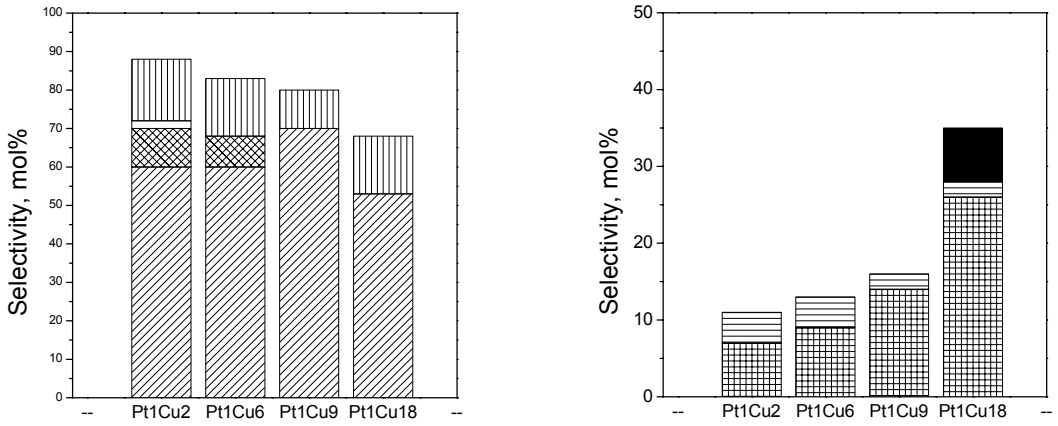

a b

Figure 3.7. Average selectivity toward C_1 products (a); and coupling products (b)for different Pt-Cu/C catalysts after initial 5min of TOS (Inclined hatched bars: CH_4; Cross hatched bars: CH_2F_2; empty bars: CH_3F; vertically hatched bars: CHF_2Cl; perpendicularly hatched bars: C_2H_4; horizontally hatched bars: C_2H_6; and filled bars: C_3H_6) (250 ^{0}C, 1 atms, CF2Cl2:H_2=1:1).

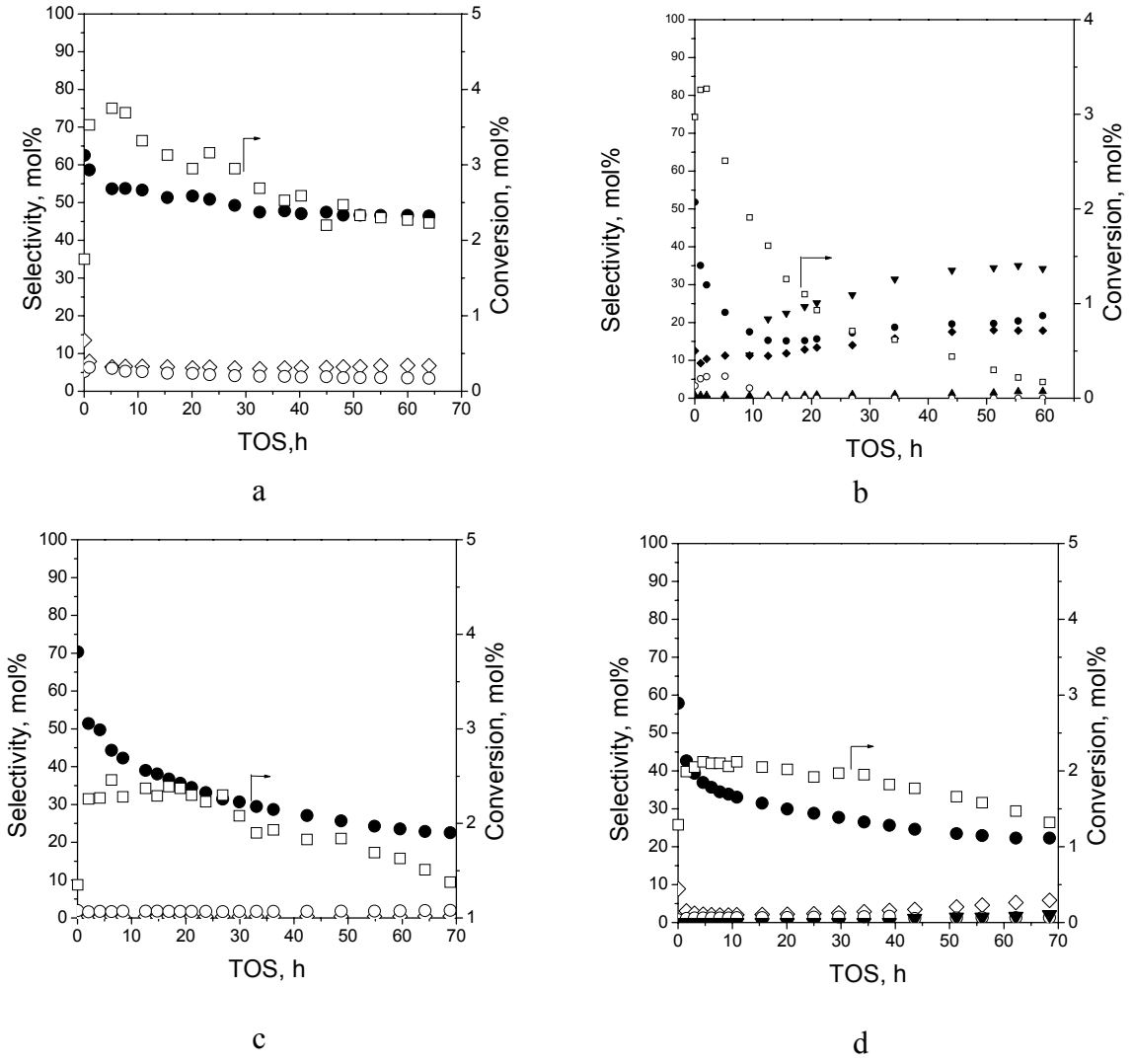

Figure 3.8 Selectivity towards C_1 products of Pt1Cu2/C (a); Pt1Cu6/C (b); Pt1Cu9/C (c); and Pt1Cu18/C (d)catalysts; CH_4 (●), CH_2FCl (▲), CHF_2Cl (◊), CH2F2 (o), CHF_3 (▼), conversion (□) (250 ^{0}C, 1 atms, CF2Cl2:H_2=1:1)

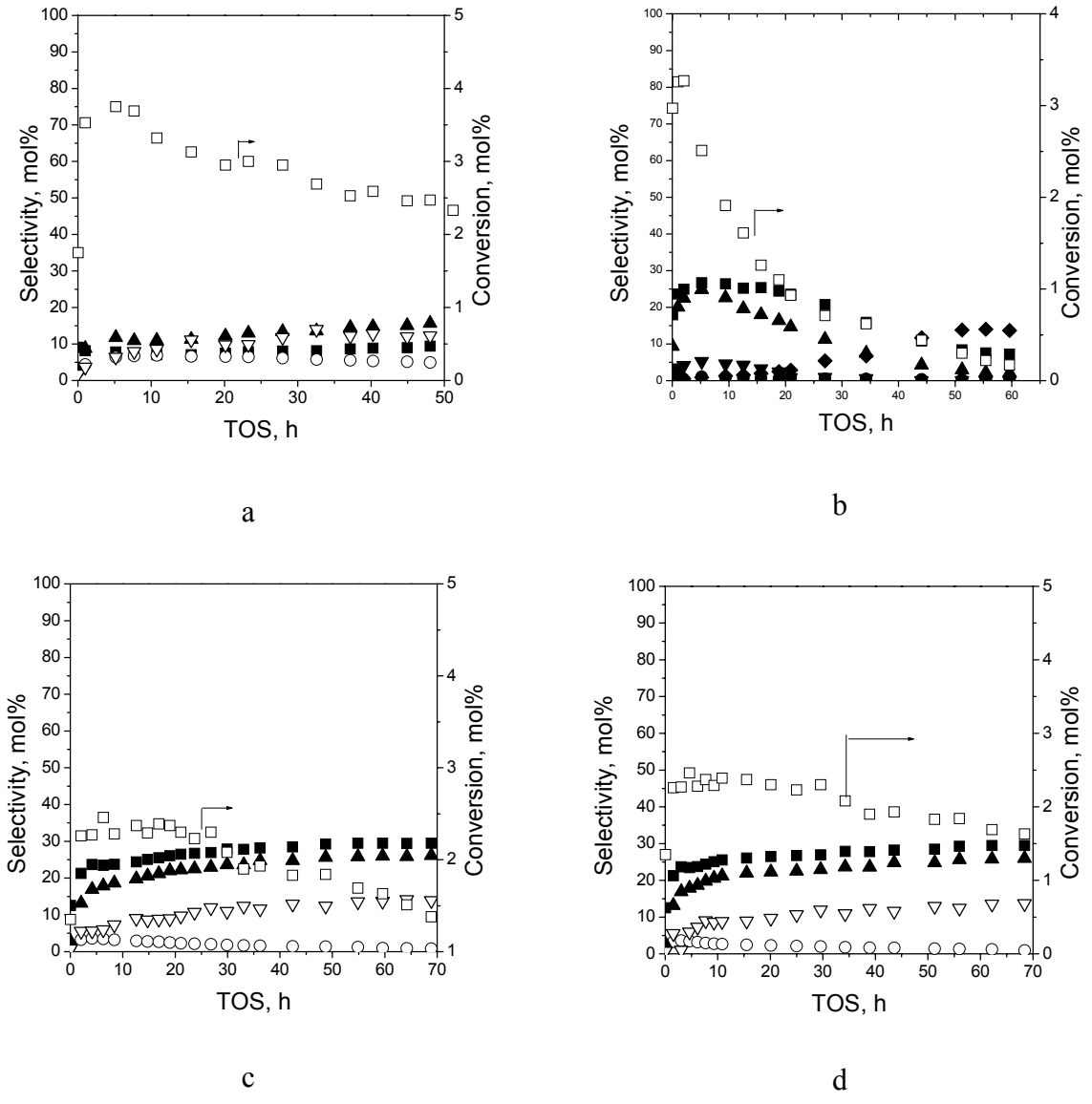

Figure 3.9 (a) Selectivity towards coupling products of Pt1Cu2/C (a); Pt1Cu6/C (b); Pt1Cu9/C (c); and Pt1Cu18/C (d)catalysts; C_2H_4 (■), C_2H_6 (o), C_2F_4 (◊), C_3 (▲), C_{4+} (∇), conversion (□) (250 ^{0}C,1 atms, CF2Cl2:H_2=1:1).

4.0 ROLE OF DIFFERENT ACTIVE SITES AND ALLOYING IN THE FORMATION OF COUPLING PRODUCTS FOR HYDRODECHLORINATION OF CF_2CL_2 ON PTCU/C BIMETALLIC CATALYSTS

4.1 Introduction

Catalytic hydrodehalogenation is one of the established ways to convert the environmentally harmful CFCs into benign and industrially useful products. Studies of hydrodechlorination of CFCs have been mainly focused on the full or partial removal of Cl atoms from the molecules to obtain alkanes or partially halogenated alkenes.[1-3] However, the production of higher molecular weight coupling products through the hydrodehalogenation of CFCs may also be possible.[4-6] It has been shown previously that Pt/C catalyst is not selective toward coupling but addition of Cu to Pt dramatically improves coupling selectivity.[7] It has been speculated that Pt sites are responsible for hydrogen dissociation and C_1 product formation whereas Cu sites are responsible for coupling products formation. However, there is no clear understanding about the roles of different active sites in the reaction.

The purpose of the work is to examine the above speculations about different active sites. Many studies have suggested the structure sensitivity of hydrodehalogenation reactions on transition metals.[8-11] If the number of Pt ensemble big enough for hydrodehalogenation were

reduced, C_1 selectivity will also go down and the selectivity toward coupling would be higher. Moreover, as H_2 dissociation on Pt is not ensemble size dependent,[12] the process will not hinder the supply of hydrogen to the Cu sites. Two methods have been used to reduce the Pt ensemble size. One is to selectively poison Pt sites by carbon monoxide (CO). The technique of selective poisoning of transition metals has been used previously by Ross and Stonehart.[13] The heats of adsorption of CO at room temperature on Pt and on Cu are 46 kcal/mol and 19 kcal/mol, respectively.[14] The large difference in the heats of adsorption means that when CO will be present in the reaction mixture, Pt sites will be preferentially occupied by CO and that will reduce the Pt ensemble size. The other possible method of Pt ensemble size reduction is exposing the fresh catalyst to water. The idea behind the technique is that the addition of water to the fresh catalyst before reduction will facilitate better mixing of the precursors and as a result the alloy formation will improve during the reduction process. Higher amounts of alloy formation mean reduction in the size of the Pt ensemble. Kinetics studies were performed using fresh catalyst, water exposed catalysts and fresh catalyst with CO in the reaction mixture to check the hypothesis that C_1 products are predominantly formed on Pt and coupling products are formed on Cu sites.

4.2 Experimental

4.2.1 Catalyst Preparation and Characterization

Activated carbon (BPL F3, 6x16 mesh, Calgon Carbon) was crushed and sieved to obtain a fraction of 24-60 mesh (1400 m^2/g surface area; 2.4 nm average pore diameter) to use as a support. The 24-60 mesh fraction was then co-impregnated with an aqueous solution of $H_2PtCl_6.6H_2O$ (Alfa, 99.9%) and $CuCl_2.2H_2O$ (MCB Manufacturing Chemists, Inc., 99%). The material was allowed to equilibrate overnight before drying at ambient temperature and pressure for 24 h. It was then dried at 100 ^{0}C for 2 h in vacuum (~25 Torr). This preparation procedure resulted in a catalyst consisting of 0.48% Pt and 0.94% Cu (the atomic ratio of Pt to Cu was 1:6) supported on activated carbon BPLF-3.

Chemisorption and BET measurements were carried out using a volumetric sorption analyzer ASAP 2010 and ASAP 2010 Chemi (Micromeritics ®). The metal-adsorbate ratio was determined from the irreversibly adsorbed CO, H_2 or O_2. The adsorbate – metal stoichiometry was assumed to be equal to 1 for CO and 2 for both H_2 and O_2. For each catalyst CO, H_2, O_2 chemisorption and titration of adsorbed oxygen with H_2 (HT) were performed sequentially with the same sample at 35 ^{0}C. Prior to measurement, the catalyst was reduced at 300^{0}C for 1 h in flowing H_2 (Praxair, 99.999%). The reduction was followed by evacuation for 1.5 h at 350 ^{0}C. Then the catalyst was cooled, the CO chemisorption was performed and the catalyst was reduced at 350 ^{0}C for 1 h and evacuated for 1.5 h at the same temperature. Next, H_2 chemisorption was conducted after which the catalyst was again evacuated at 350 ^{0}C for 1.5 h. This was followed

by O_2 chemisorption, evacuation at 350 ^{0}C for 1 h and H_2 titration. The dispersion results are shown in Table 4.1.

The catalyst exposed to water was prepared by adding 10 drops of water to 500 mg of fresh catalyst and shaking vigorously until the water mixed well with the catalyst. The water treated catalyst was stored airtight for at least a week to equilibrate.

4.2.2 Catalytic Experiments

The hydrodechlorination of CF_2Cl_2 (Atochem, purity >99%; detectable impurities: CHF_2Cl ~0.25% and CH_3CF_3 ~0.25%) was conducted at atmospheric pressure in a stainless steel flow reaction system consisting of a down-flow quartz micro reactor (10 mm i.d.) equipped with a quartz frit to support the catalyst. An electric furnace was used to heat the reactor zone containing the catalyst. The catalyst bed temperature was measured and controlled with an accuracy of ± 1 ^{0}C (Omega model CN2011). The gas flows (CFC, H_2, Praxair, purity 99.9%; He, Praxair, purity 99.9%; CO, VWSCO, 4% balance He) were metered with mass flow controllers (Brooks Instruments, model 5850E) and mixed prior to entering the reactor. The reactor effluent was analyzed by on-line GC and by GC/MS to identify the reaction products. The GC (HP 5890 series II) was equipped with a 15 ft 60/80 Carbopack B/5% Fluorocol packed column (Supelco) and a flame ionization detector (FID) capable of detecting concentrations >1 ppm for all CFCs, chlorocarbons and hydrocarbons under investigation. The on-line HP GC/MS system consisted of a HP 5890 series II Plus GC equipped with a Fluorocol column connected to a HP 5972 Mass Selective Detector.

Prior to reaction, the catalyst was treated with a mixture of H_2 (20 ml/min) and He (30 ml/min) as it was heated from 27 ^{0}C to 400 ^{0}C at a rate of 5 ^{0}C /min and then held at 400 ^{0}C for 120 min. The catalyst was cooled in flowing He (30 ml/min) to the reaction temperature, 250 ^{0}C, and the reactant mixture was introduced. The reaction was conducted at a CF_2Cl_2 to H_2 molar ratio of 1 (2 ml/min of each) with He (26 ml/min) as diluent. The CF_2Cl_2 to H_2 molar ratio used in this work is the stoichiometric ratio required for the dechlorinative dimerization of CF_2Cl_2 to C_2F_4. In all cases the conversion was kept below 5 % to maintain condition for ideal differential reactor. All experiments were stopped after the conversion had reached to < 0.2 %.

The selective CO poisoning was done by flowing 4% CO in He at a rate of 2 ml/min with the reaction mixture. Total flow rate was kept constant at 30 ml/min by reducing the He flow rate accordingly.

For all the experiments the total flow rate was 30 ml/ and the catalyst weight was ~0.03 g. The selectivities (S_i) toward detectable carbon-containing products were calculated as follows:

$$S_i = \frac{n_i C_i}{\sum_i n_i C_i}$$

where n_i and C_i are the number of carbon atoms in a molecule and the mole concentration of the product i in effluent gas respectively. The formation of HCl was detected by GC/MS but not quantified.

The reaction rates per gram of catalyst was calculated by applying the differential reactor approximation in the form

Rate (mmol/gsec)= F∗y/W,

where F is total molar flow rate, y is the mole fraction of reactant converted, and W is the catalyst weight. The turnover frequencies (TOF) were calculated using the expression

$$TOF\ (s^{-1}) = R * MW_{Pt} / M * d.$$

where R is the rate per gram of catalyst, MW_{Pt} is the molecular weight of Pt, M is the Pt loading percent, and d is the dispersion.

4.3 Results

In comparison to the Pt/C catalysts, the selectivity toward the coupling products was substantially higher for the PtCu/C catalyst,the PtCu/C catalyst that was treated with water, and the PtCu/C catalyst that was exposed to CO during the reaction. The results shown in Figure 4.1 correspond to the maximum selectivity toward coupling for each catalyst. It is worth mentioning that the coupling selectivity for changed with TOS. These maxima were obtained at different time on stream (TOS): 5 h for PtCu/C, 0.03h for PtCu/C when CO is present in the reactants, 34 h for water exposed PtCu/C. The coupling selectivity for Pt/C was < 2% with ethane as only detectable coupling product and the selectivity remains unchanged with TOS.[15] For the PtCu/C catalyst the coupling selectivity was ~58% with a product distribution of 26.7% ethene, 1% ethane, 25% propene, 5% C_{4+} and the remaining 42% were C_1 products. When CO was present in the reaction mixture, the maximum selectivity toward coupling products increased ~69%. The main coupling products when CO was present in the reaction mixture were ethylene ~40%, propene ~24% and C_{4+} ~5%. Water exposure to the fresh catalyst increased the coupling

selectivity to ~85% with a coupling product distribution of ethylene ~34%, ethane ~2%, propene ~32% and C_{4+} ~15%.

As mentioned above, the products selectivity for the bimetallic catalyst changed as a function of TOS (Figure 4.2). With PtCu/C catalyst, the initial selectivity toward CH_4 was ~50% and decreased to ~18% after 20 h of TOS before increasing to 28% after 68 h of TOS. The formation of trifluoromethane (CHF_3) was detected only after approximately 10 h of TOS with a selectivity of ~20%. The selectivity toward CHF_3 increased from ~20% to ~38% between 10h and 68 h of TOS. Difluoromethane (CH_2F_2) was detected during the initial 10 h of TOS with a maximum selectivity of 5% after approximately 5 h of TOS and decreased thereafter to a negligible amount. The selectivity toward the other C_1 product, CHF_2Cl was initially ~15%. After 50 h of TOS the selectivity increased to ~18% and then a continuous decrease was observed to reach a selectivity of ~ 10 % after 68 h of TOS. The selectivity distribution for the coupling products formed on the PtCu/C catalyst is shown in Figure 4.2b. The selectivity toward C_2H_4 was ~20% initially, went to a maximum of ~27% after approximately 5 h of TOS before decreasing to ~8 % after 68 h of TOS. The selectivity toward C_3H_6 initially was ~20%, reached a maximum of 25% after approximately 5 h of TOS before decreasing to zero after 60 h of TOS. The maximum selectivity toward C_{4+} products was ~5% after 5 h of TOS. No C_{4+} was detected after 20 h of TOS. Tetrafluoroethylene (C_2F_4) was detected only after 20 h of TOS and reached a maximum selectivity of ~15% after 60 h of TOS before decreasing to ~10% after 68 h of TOS.

Whereas the PtCu/C catalyst maintained a conversion >0.2% for approximately 10 h of TOS, the conversion decreased to less than 0.2% in 20 h when CO was present in the reaction mixture. Two C_1 products were formed from the reactants when CO was added to the stream: CHF_3 and CHF_2Cl (Figure 4.3a). The selectivity toward CHF_2Cl initially was ~25 % and

increased monotonically with TOS to ~30% after 20 h. Trifluoromethane was detected after approximately 3 h of TOS with a selectivity of

~18 %. The CHF_3 selectivity increased gradually during 3-10 h of TOS to ~50% and remained constant thereafter. The selectivity toward coupling products formed when CO was present in the reactant stream is shown in Figure 4.3b. The selectivity toward C_2H_4 was ~40%initially and decreased monotonically to ~5% after 20 h of TOS. The propylene selectivity, which was ~25% initially, decreased to zero after approximately 12 h of TOS. The selectivity toward tetrafluoroethylene increased continuously with TOS from 0 to ~20% after 20 h of TOS.

The selectivity distribution for the water-exposed catalyst showed was not a strong function of TOS and the conversion did not decrease below 0.2% for more than 70 h. The C_1 products of significant selectivity were CHF_2Cl and CHF_3. The selectivity toward CHF_2Cl initially was ~25% and decreased to ~11% after 65 h of TOS. The CHF_3 selectivity increased from 0 to ~8.5% after 65 h of TOS (Figure 4.4a). The main coupling products for water-exposed catalyst were ethylene and propylene. The ethylene selectivity was ~49% initially before decreasing to ~40% within approximately 3 h and remaining constant thereafter. The selectivity toward propylene was ~18% initially, increased to ~32% after 10 h of TOS and remained essentially constant thereafter. The initial selectivity toward C_{4+} was ~0%, reached to a maximum ~16 % after approximately 25 h of TOS before decreasing to ~12% after 65 h of TOS. The selectivity toward C_2H_6 was ~5 % initially and decreased to a negligible value after ~25 h of TOS. C_2F_4 was also detected but the selectivity was less than 2% for the entire reaction period.

Catalyst exposure to water changed the activity and deactivation rate significantly in comparison to the catalyst not exposed to water (Figure 4.5). The initial conversion of the fresh catalyst and the water-exposed catalyst were ~3 and ~0.6 mol%, respectively. However the fresh

catalyst deactivated very rapidly within first 30 h of TOS. After approximately 15 h of TOS the activity for fresh catalyst became less than that of the water-exposed catalyst. There was almost no further deactivation for both the catalysts after approximately 30 h of TOS.

4.4 Discussion

The result of CO poisoning experiment showed higher coupling selectivity at the very beginning of the reaction but gradually dropped down with TOS. The catalyst also lost its activity with a very short period (~20 h compared to ~70 h for catalyst without poisoning). The most interesting result is the selectivity increase of fluorinated C_1 halocarbons (CHF_3 and CHF_2Cl) and coupling products ($CF_2=CF_2$). There can be two reasons behind these phenomena. Carbon monoxide blocks Pt sites as well as more active Cu or bimetallic sites. In CF_2Cl_2 the difference between gas phase bond energy (318 and 460 kJ/mol for C-Cl and C-F bonds, respectively) suggest that sites with higher heats of adsorption will be required to break C-F bond. As a result of the blockage of theses high energy sites by CO the C-F bond might not be broken, which gives rise to more surface $:CF_2$ species. The other factor is the competition between CO and H_2 for adsorption sites. On Pt(111) the heat of adsorption for CO ranges between 140 kJ/mol for low coverage to 40 kJ/mol for saturation coverage.[16] For hydrogen the heat of adsorption on the same surface remains constant around 40 kJ/mol.[16] Therefore a competition for adsorption sites between these two molecules is logical. Whatever is happening, CO will mainly affect the performance of Pt or bimetallic sites and the Cu sites will probably

remain intact. Therefore, it can tentatively be concluded that hydrogenolysis or rapture of C-F requires mainly Pt or bimetallic Pt-Cu sites.

Exposing the calcined catalyst to water showed a very significant improvement in both stability and coupling selectivity of the catalyst. This can be due to improved alloy formation. Considering the large surface area of the carbon support and low metal loading (<1.5%), it can be speculated that the metal precursors will be highly dispersed on the support surface. Due to the specific adsorption on the supporting surface, one or both of the components might be strongly anchored to the surface, the mixing of the constituent should, therefore, be achieved either during calcinations or reduction. For the PtCu bimetallic catalyst alloy formation can be thought of by the 'catalyzed reduction model'[17] where Pt particles are formed first because of the easy reducibility, and then mobile Cu^{2+} ions are adsorbed by these Pt particles and swiftly reduced. The activation of hydrogen by the noble metal and the migration of the activated hydrogen to the less reducible element may also be another reason for the reducibility enhancement. There are abundant reports in the literature about the presence of a noble metal can enhance the reduction of ions of a less reducible element.[18-25] However, for this process to occur, the less reducible ions need to be in close proximity of either the ions or the reduced nuclei of the more noble metals.[26]

Addition of water to the calcined catalyst can improve the mobility of the catalyst precursors.[26] This can be due to the formation of a mobile Cu aqeuo complex. This induce mobility enables the $[Cu(H_2O)_6]^{2+}$ ions migrate towards the Pt ions and fulfill the proximity requirements for enhanced reducibility and bimetallic particle formation. Therefore the exposure of the calcined catalyst to water might improve the proportion of alloying in the bimetallic catalyst. The kinetics results can now be considered based on the above conclusion.

The main speculation of improved coupling selectivity on Pt-Cu/C bimetallic catalyst is the dual site mechanism: the Pt sites will be used as source of activated hydrogen and hydrodehalogenation and coupling will take place on Cu sites.[27-28] For this to happen, the ideal surface would be like minimum number of Pt atoms required for dissociating hydrogen surrounded by Cu atoms. As the degree of alloying increases, the chances of higher proportion of the above mentioned surface increase. This will ensure that there is enough hydrogen to clean the Cu surface as well as hydrogenate C-F bonds to form surface :CH_2 species. The significant improvement in the stability of the water-exposed catalyst can also be explained by the lowering of Pt ensemble size (Figure 4.5). Deactivation during the reaction of hydrodechlorination on Pt/C catalyst has been related to the formation of chlorine containing carbonaceous deposits on the metal.[29] As Cu does not form bulk carbide,[30] deactivation of Cu sites by carbonaceous deposits is possibly unlikely. If the Pt ensemble size is small, there will be less probability of carbonaceous deposit formation because there will not be enough adjacent sites present to form multiple C-Pt bonds necessary for carbonaceous deposit.

4.5 Conclusion

The role of different active sites and alloying in the reaction of CF_2Cl_2 and H_2 on Pt-Cu/C were investigated in this chapter. Carbon monoxide was introduced in the reaction mixture. The maximum coupling selectivity was increased from 55% to 69%. It was suggested that CO decreases the ensemble sizes of Pt by poisoning the active sites. The catalyst was also exposed to water for better mixing of the precursors. The water-exposed catalyst showed an overall

coupling selectivity of 90% and the performance was very stable. It was suggested that water exposure of the fresh catalyst increases bimetallic particle formation. As a result the number and size of monometallic Pt particles decrease. Both the results point towards the fact that Pt or bimetallic sites may be responsible for C_1 product formation and Cu sites are responsible for coupling products formation.

Table 4.1. Irreversible Gas Uptake and Apparent Dispersion

Catalyst composition (wt%)	Pt/Cu (at. ratio)	Uptake (μmol/g_{cat}) CO	H_2	O_2	H_2 (HT)	Apparent dispersion (%) CO/ Pt_t	H/Pt_t	O/ $(Pt+Cu)_t$	H/Pt_t (HT)
Support	-	0	0	3.0	0	-	-	-	-
0.49% Pt	∞	6.8	0.2	9.0	8.5	26.5	1.7	70.5	66.4
0.48%Pt+ 0.95% Cu	1:6	11.0	0.4	23.3	1.9	44.8	3.0	26.8	15.4

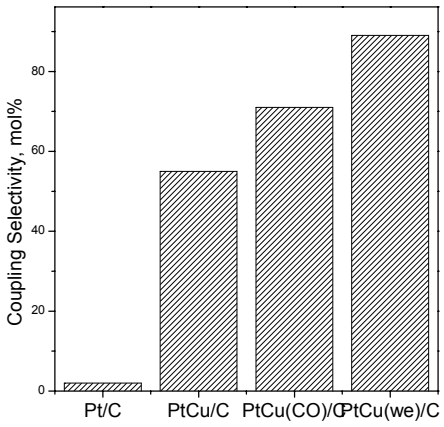

Figure 4.1 Maximum selectivity toward coupling products for Pt and PtCu/C catalysts; (we: water exposed catalyst, CO: presence of CO in the reaction mixture) (250 ^{0}C, 1 atms, CF_2Cl_2: H_2 = 1:1).

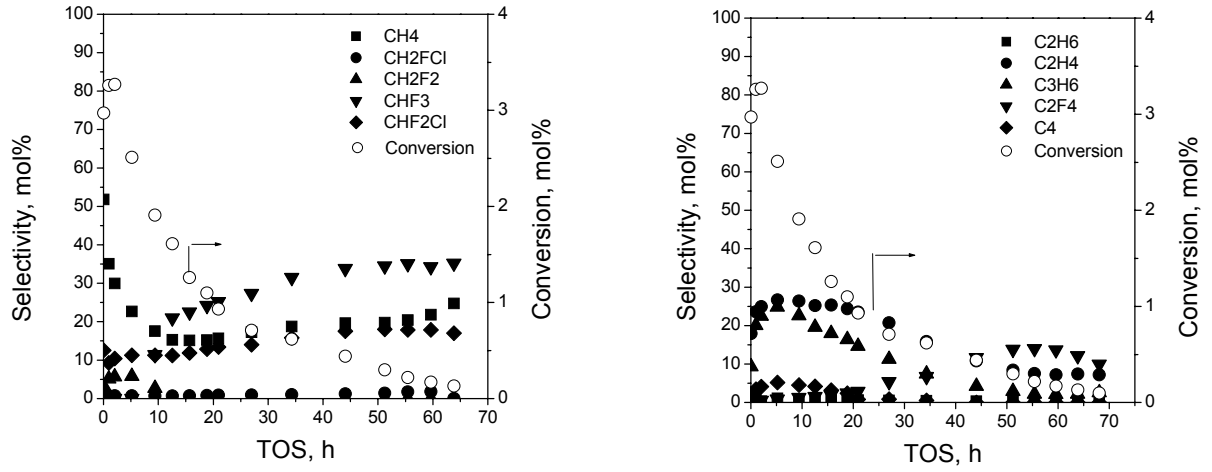

a b

Figure 4.2. Selectivity toward C_1 products (a); and C_2 products of PtCu/C catalysts (b) (250 ^{0}C, 1 atms, CF_2Cl_2: H_2 = 1:1).

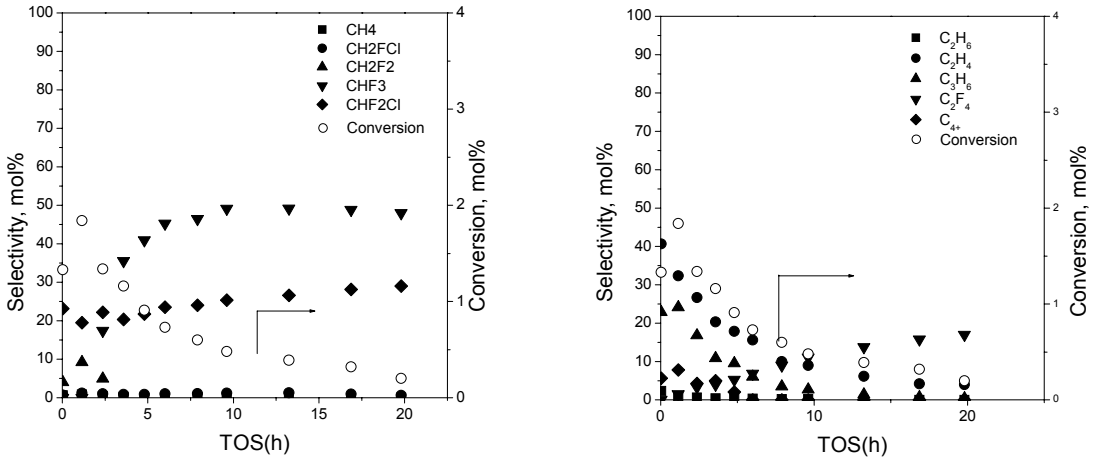

a b

Figure 4.3 Selectivity toward C_1products (a) ; and C_2 products (b) of PtCu/C catalysts when CO was present in the reaction mixture (250 ^{0}C, 1 atms, CF_2Cl_2: H_2 = 1:1).

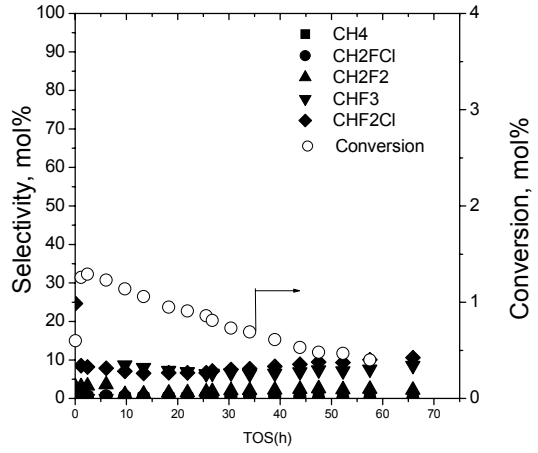

a

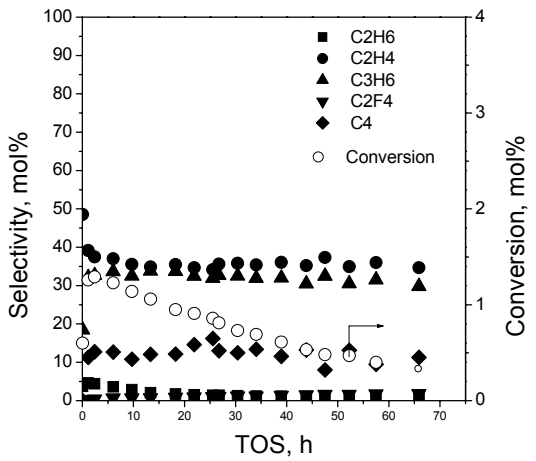

b

Figure 4.4 Selectivity toward C_1 products (a); and C_2 products (b) of water-exposed PtCu/C catalysts (250^0C, 1 atms, CF_2Cl_2: H_2 = 1:1).

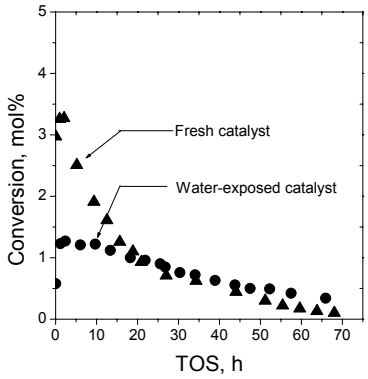

Figure 4.5 TOS profile of reaction rates for fresh (▲) and water-exposed (●) catalysts (250 ^{0}C, 1 atms, CF_2Cl_2: H_2 = 1:1).

5.0 HYDRODEHALOGENATION OF DICHLORODIFLUOROMETHANE ON PALLADIUM BIMETALLIC CATALYSTS SUPPORTED ON ACTIVATED CARBON BPL F3

5.1 Introduction

Halocarbons can be interesting intermediate to produce carbon-carbon coupling products like ethylene and propylene.[1-3] Halocarbons are known environmental pollutants[4] and most of the investigations to convert those to environmentally benign and useful products by reacting with hydrogen on a catalyst concentrate on selectively replacing Cl atoms from the molecules by hydrogen to produce hydrofluorocarbons.[5-8] Coupling products were observed as byproducts of hydrodechlorination reactions of dichlorodifluoromethane(CF_2Cl_2) catalyzed by transition metals such as Pt,[9] Pd, [5,10,11] Ru,[12,13] Os,[13] Ni, Co and Fe.[14,15] A specific investigation devoted to the coupling of CF_2Cl_2 catalyzed by activated carbon supported Group VIII noble metals (Pt, Pd, Ru, Rh, Os, and Ir) at 523 K in the presence of H_2 showed that the Pd/C catalyzed the formation of C_2 and C_3 hydrocarbons with ~75 mol% selectivity and C_2H_4 (~40 mol%) as the major coupling product. The Ru, Rh, Os, and Ir/C catalyzed the formation of fluorinated coupling products (CF2CF2 and CF_2CH_2), but the selectivity toward these compounds was less than 5 mol% in each case.[16] So, the main challenge to form coupling products from halocarbons is to

lower the energy barrier for the coupling pathways by using a proper catalyst so that the byproducts become the main products.

Though it has long been known that alloying significantly changes the catalytic properties,[17-19] it is still a matter of debate whether this change is due to ensemble effects,[20,21] structure effects,[21] or electronic effects.[23] Using alloy catalysts creates the opportunity to tune the catalyst properties to achieve the desired results. Carbon supported Pt showed less than 5 mol % selectivity toward coupling products formation in the reaction of CF_2Cl_2 and H_2 but when Cu or Co was added to Pt, the coupling selectivity increased 10 times.[24] Tetrafluoroethylene was observed with PdFe/graphite and PdCo/graphite catalysts during the CF_2Cl_2 +H_2 reaction at high CFC to H_2 ratios, whereas Pd/graphite catalyst did not show any selectivity toward coupling products.[25] Even though carbon supported monometallic Ni catalyst exhibited 33 mol% selectivity toward C_2 compounds in the same reaction, modifying the Ni/C with Al and Cu increased the coupling selectivity to 43 and 46 mol%, respectively.[26]

One of the purposes of using alloy catalysts is to extract the intrinsic properties of individual metals to improve the selectivity toward the desired reaction path. The group IB metals (Cu, Ag) and the group VIII metals (Fe, Co) are the potential candidates for the coupling of the surface carbene and fluorocarbene species formed in the reaction of CF_2Cl_2 and H_2. Copper and Ag can break C-X bonds.[27-29] Also, these group IB metals favor desorption of hydrocarbons species from the catalyst surface, rather than further degradation, increasing the probability of coupling of those fragments to produce higher molecular weight compounds.[28,29] However, the group IB metals do not dissociate H_2 readily[30] and one cannot expect that they will show high activity in CF_2Cl_2 + H_2 reaction. Iron and Co are Fischer-Tropsch catalysts that produce higher molecular weight hydrocarbons from CO and H_2.[31] Even though both Fe and

Co can dissociate H_2, partial coverage of the surface with halogen atoms may significantly suppress H_2 activation. Therefore, another metal such as Pt or Pd that can dissociate H_2 readily is necessary to keep the group IB and group VIII metals active in the atmosphere containing HCl and HF.

The objective of the present investigation is to test the hypothesis that alloying IB metals like Cu and Ag, and VIII metals like Co and Fe, all of which have C-C coupling ability but inactive in the severe environment of hydrodehalogenation, can be alloyed with Pd to convert them to active catalysts for the reaction of $CF_2Cl_2 + H_2$ to produce

C-C coupling products. The main hypothesis is that Pd would serve as a source of dissociated H_2, which will migrate to the second metal sites by spill over to clean the metal of adsorbed Cl and F. The hydrodehalogenation activity of Pd will be suppressed by the dilution effect of the second metal because of the structure sensitivity of the reaction.[32-34]

5.2 Experimental

5.2.1 Catalyst Preparation

Activated carbon (BPL F3, 6x16 mesh, Calgon Carbon) was crushed and sieved. A fraction of 24-60 mesh (1400 $m^2 \cdot g^{-1}$ surface area; 24 Å average pore diameter) was used as a support. The support was co-impregnated with an aqueous solution of $PdCl_2$ (Aldrich Chemical Co., 99.9%, metals basis) and one of the following metal chloride solutions: $CuCl_2 \cdot 2H_2O$ (MCB Manufacturing Chemists, Inc., 99%), $CoCl_2 \cdot 6H_2O$ (Fisher Scientific, 100%) and $FeCl_3 \cdot 6H_2O$ (Avocado Research Chemicals Ltd., 99%). In each case the mixture was allowed to equilibrate overnight and was dried at ambient temperature and pressure for 24 h and then at 373 K for 2 h in vacuum (~25 Torr). The weights of metal chlorides were selected such that the molar ratio of Pd to the second metal was 1:6. The Pd-Ag/C catalyst was prepared by sequential impregnation of the support. The aqueous solution of $AgNO_3$ (Alfa AESAR, 99.9995%, metals basis) was used first to impregnate Ag on the support followed by the drying step and a second impregnation step with $PdCl_2$ solution. The catalyst compositions are listed in Table 5.1.

The catalysts were exposed to water by adding 10 drops of water to 500 mg of fresh catalyst and shaking vigorously until the water mixed well with the catalyst. The water treated catalyst was stored airtight for at least a week to equilibrate.

Chemisorption measurements were conducted with a volumetric sorption analyzer (Micromeritics® ASAP 2010 Chemi). The metal-adsorbate ratio was determined from the irreversibly adsorbed CO, H_2 or O_2. The adsorption stoichiometry was assumed to be 1 for CO

and 2 for both H_2 and O_2.[24] For each catalyst CO, H_2, and O_2 chemisorption as well as titration of adsorbed oxygen with H_2 (HT) were performed on the same sample at 308 K and pressures of 100-800 Torr. Prior to making these measurements the catalyst was reduced in flowing H_2 at 573 K for 2 h and at 673 K for 1 h. This was followed by evacuation for 1.5 h at 673 K. The catalyst was then cooled and CO chemisorption was performed before the catalyst was reduced at 673 K for 1 h and evacuated for 1.5 h at the same temperature. Then the H_2 was chemisorbed and the catalyst was again evacuated at 673 K for 1.5 h. This was followed by O_2 chemisorption, evacuation at 308 K for 1 h and H_2 titration.

5.2.2 Catalytic Experiments

The hydrodechlorination of CF_2Cl_2 (Atochem, purity >99%; detectable impurities: CHF_2Cl ~0.25% and CH_3CF_3 ~0.25%) was conducted at atmospheric pressure in a stainless steel flow reaction system consisting of a down-flow quartz microreactor (10 mm i.d.) equipped with a quartz frit to support the catalyst. An electric furnace heated the reactor zone containing the catalyst. The catalyst bed temperature was measured and controlled with an accuracy of ± 1 K (Omega model CN2011). The gas flows (CFC, H_2, Praxair, purity 99.9% and He, Praxair, purity 99.9%) were metered with mass flow controllers (Brooks Instruments, model 5850E) and mixed prior to entering the reactor. The reactor effluent was analyzed by on-line GC and by GC/MS to identify the reaction products. The GC (HP 5890 series II) was equipped with a 15 ft 60/80 Carbopack B/5% Fluorocol packed column (Supelco) and a flame ionization detector (FID) capable of detecting concentrations >1 ppm for all CFCs, chlorocarbons and hydrocarbons under

investigation. The on-line HP GC/MS system consisted of a HP 5890 series II Plus GC equipped with a Fluorocol column connected to a HP 5972 Mass Selective Detector.

Prior to reaction, the catalyst was treated with a mixture of H_2 (20 ml/min) and He (30 ml/min) as it was heated from 300 K to 673 K at the rate of 5 K/min and then held at 673 K for 120 min. The catalyst was cooled in flowing He (30 ml/min) to the reaction temperature, 523 K, and the reactant mixture was introduced.

The reaction was conducted at a CF_2Cl_2 to H_2 ratio of 1 (2 ml/min of each), the stoichiometric ratio required for the dechlorinative dimerization of CF_2Cl_2 to C_2F_4. During all the experiments the total flow rate used was 30 ml/min (balance He) and the catalyst weight was ~0.1 g. The selectivities (S_i) toward detectable carbon-containing products were calculated as follows:

$$S_i = \frac{n_i C_i}{\sum_i n_i C_i}$$

where n_i and C_i are the number of carbon atoms in a molecule and the mole concentration of the product i in effluent gas respectively. The formation of HCl was detected by GC/MS but not quantified.

5.3 Results

5.3.1 Dispersion Measurements

The results of chemisorption measurements on carbon supported monometallic Pd, and bimetallic catalysts, as well as on the pure support are listed in Table 5.1. As all chemisorption measurements have some drawbacks, four types of experiments were done so that a comparison could be made. The uptake of hydrogen was negligible for all catalysts. Palladium and the other metals chemisorb O_2; however, the stoichiometry of O_2 chemisorption on transition metals is sufficiently dubious that the oxygen uptake results could not be used as an independent measure of dispersion. In addition, Pd can catalyze the oxidation of the carbon support during O_2 chemisorption measurements increasing irreversible oxygen uptake. While CO chemisorption on Pd is well defined, metallic Ag does not chemisorb CO, while CO chemisorption is reversible on Cu.[24] Both Co and Fe chemisorb CO irreversibly, but the adsorption stoichiometry varies in a wide range depending upon support, metal loading and preparation. Hence, the titration of pre-adsorbed oxygen with gaseous H_2 (HT) according to the stoichiometry,

$$PdO + 3/2\ H_2 \longrightarrow PdH + H_2O$$

was the most accurate method to determine the fraction of Pd atoms exposed in the catalysts used in the present investigation, and the HT data were used for the turnover frequency (TOF) calculations. It was shown in separate experiments that none of the Cu, Ag, Fe and Co catalysts were capable of reducing adsorbed oxygen with H_2 at 308 K suggesting that the uptake of H_2 in the HT experiment corresponded only to Pt atoms on the surface of the catalyst.

5.3.2 Time on Stream Behavior

The Pd/C as well as the bimetallic catalysts containing Pd with Cu, Ag, Fe or Co deactivated with time on stream (TOS) during the reaction of CF_2Cl_2 and H_2 at 523 K (Figure 5.1). The maximum conversions were in the range 3.5-20 mol% at early TOS. After 45 h of TOS Pd, Pd-Cu, Pd-Co, Pd-Fe/C, and Pd-Ag/C lost ~66%, ~50%, ~72%, ~42%, ~93% of their maximum activity, respectively.

The reaction products were separated in two categories: the coupling or C_{2+} products and C_1 products with varying degree of dehalogenation. Figure 5.2b shows the selectivity of C_{2+} products formed on monometallic Pd/C as a function of TOS. The Pd/C catalyst showed ~60 mol% initial selectivity toward hydrocarbon coupling products; the selectivity toward C_2H_4, C_2H_6, C_3 and C_{4+} products was ~15 mol% each. After 120 h of TOS the total selectivity toward hydrocarbon coupling products was ~80 mol%. The C_2H_4 selectivity increased from 15 to 38 mol% and the C_2H_6 selectivity decreased from 15 to 5 mol% during 120 h of TOS. Higher hydrocarbons C_3 (15-20 mol%) and C_4+C_5 (~15 mol%) were produced at all the TOS. However, halogenated coupling products were not observed on this catalyst.

Addition of Cu to Pd resulted in formation of C_2H_4 as the only major coupling product (Figure 5.3a). The initial selectivity toward hydrocarbon coupling products on the Pd-Cu/C was ~75 mol%; C_2H_4 (~65 mol%), C_2H_6 (~5 mol%) and C_3 (~10 mol%) were the major coupling products during initial 1 min of TOS. However, the selectivity of C_2H_4 decreased from a maximum of ~75 mol% to ~40 mol% after 70 h of TOS. C_2H_6 selectivity dropped to zero after 20 h TOS. The selectivity toward C_3 dropped from a maximum of 10 mol% after 1h to 5 mol% after 70 h.

Pd-Ag/C showed the highest selectivity toward C_2H_4 and then toward the halogenated coupling product C_2F_4 (Figure 5.3b). The C_2H_4 selectivity was ~43 mol% at the beginning, decreased to 18 mol% after 20 h of TOS and after that started increasing to reach 25 mol% after ~48 h of TOS. The selectivity toward C_2F_4 increased to ~10 mol% after ~48 h of TOS. C_3 was also produced during entire reaction time but the selectivity decreased from ~11 mol% at the beginning to 5 mol% after ~48 h of TOS.

The Pd-Co/C catalyst showed high selectivity toward hydrocarbon coupling products and the product distribution was very stable (Figure 5.3c). The initial selectivity towards coupling product was ~57%; C_2H_4 (~25 mol%), C_2H_6 (~22 mol%), and C_3 (10 mol%) were the major coupling products. After 70 h of TOS the total hydrocarbon oligomerization selectivity was 65 mol%; C_2H_4 (~35 mol%) and C_3 hydrocarbons (~25 mol%) were the major products.

The highest selectivity toward oligomerization products was obtained with Pd-Fe/C bimetallic catalyst (Figure 5.3d). The initial selectivity toward hydrocarbon coupling products was 64 mol%; C_2H_4 (~47 mol%), C_2H_6 (~5 mol%), C_3 (~5 mol%), C_{4+} (~2 mol%), C_5 (~5 mol%) were the major coupling products. After 68 h of TOS, selectivity toward C_2H_4 increased to 35 mol%, selectivity toward C_3 increased to 25 mol%, selectivity toward C_2H_6 increased to ~15 mol% and selectivity toward C_4 increased to ~10 mol%.

Palladium showed overall low selectivity toward C_1 products (25 mol%) as compared to coupling products (75 mol%) (Figure 5.2a). The selectivity toward CH_2F_2 decreased from 30 to 10 mol% over 120 h of TOS while those of other C_1 products remained unchanged during the course of the reaction. The other C_1 products were CHF_2Cl (8 mol%), CH_4 (5 mol%, CH_3F and CHF_3 (2 mol% each).

For all the bimetallic catalysts except Pd-Ag/C the major C_1 products were CH_2F_2 and CHF_2Cl. The PdAg/C catalyst produced CHF_3 as the major C_1 product with a maximum selectivity of ~45 mol% (Figure 5.4b). The selectivity toward CHF_2Cl was ~26 mol% at the beginning and decreased to ~15 mol% and the selectivity toward CH_2F_2 increased from zero at the beginning to ~11 mol% after ~48 h of TOS. For PdCu/C the selectivity toward CH_2F_2 increased from ~1 mol% to ~40 mol% and that toward CHF_2Cl was 25 % after 1 min of TOS and increased to ~10 mol% after 70 h of TOS (Figure 5.4a). For PdCo/C catalyst the selectivity toward CH_2F_2 was 17 mol% at the beginning and decreased to ~12 mol% after 80 h after reaching a maximum of ~23 mol% after ~1h of TOS (Figure 5.4c). The selectivity toward CHF2Cl was ~23 mol% at the beginning, decreased to ~16 mol% after ~6h and then increased to ~23 mol% after 80h of TOS. PdFe/C showed the lowest C_1 selectivity of all the catalysts after ~5h of TOS; the combined C_1 selectivity was ~15 mol% with ~7 mol% for CHF_2Cl and ~8 mol% for CH_2F_2 (Figure 5.4d).

5.4 Discussion

Palladium is one of the most favored metals for hydrodehalogenation of CFCs. At a high H_2 to CF_2Cl_2 ratio CH_2F_2 was the major product.[35-41] However, the results of the reaction of H_2 and CF_2Cl_2 on Pd/C discussed in the paper showed C-C coupling compounds (~75 mo%) as major products. It was speculated that electron deficient Pd formed on the acidic support lead to a weak interaction between $:CF_2$ species and Pd, helping the fluorocarbene species to desorb after interacting with surface H atoms to produce CH_2F_2.[42] However, Pd supported on activated carbon will not probably become electron deficient because of the inert nature of the support. Moreover, It was suggested that poorly dispersed Pd particles enhance CH_2F_2 selectivity by forming Pd-carbide phase. Smaller particles are less prone to carbiding because of the lower proportion of plane atoms.[43] The inability to detect the Pd particles using XRD and TEM and the high surface area of the activated carbon support suggest that the Pd particle size in the catalyst used in the current investigation is of the order of 1 nm. Small Pd particles (1.5-2 nm) supported on carbon (Sibunit) produced C-C coupling products (~40%) during the reaction of CCl_4 and H_2 at 150-230^0 C.[44] Based on the above observations, it can be concluded that the small Pd particle size might be one of the reasons of higher coupling products selectivity of the catalyst. Moreover, one must also consider the fact that a higher CCl_2F_2/H_2 ratio (1 vs. 0.35 used by Coq et al. and 0.35 used by Juszczyk et al.) was used in the experiment. Higher concentration of CF_2Cl_2 will probably give rise to a higher surface concentration of carbene species, which in term will couple instead of desorbing from the surface by reacting with H. Coq et al. have related the formation of C_2F_4 on PdFe/graphite and PdCo/graphite from the reaction of H_2 and CF_2Cl_2 to the higher concentration of $*CF_2$ surface intermediates.[35]

Addition of IB metals, Cu or Ag that are inactive for the reaction showed a drastic decrease in catalyst activity (Figure 5.1) but the bimetallic catalysts were more stable than the monometallic Pd catalyst. Addition of group VIII metals Fe or Co to Pd also decreased the activity and made the catalyst more stable but the effect was less pronounced in case of Fe. The addition of a second metal to Pd has a significant effect on morphology and surface characteristics of the particles. Considering the large surface area of the carbon support and low metal loading (<2%), it can be speculated that the metal precursors will be highly dispersed on the support surface. Due to the specific adsorption on the supporting surface, one or both of the components might be strongly anchored to the surface, the mixing of the constituent should, therefore, be achieved either during calcinations or reduction. For the Pd-M bimetallic catalyst alloy formation can be thought of by the 'catalyzed reduction model'[45] where Pd particles are formed first because of the easy reducibility, and then mobile second metal ions are adsorbed by these Pd particles and swiftly reduced. Obviously one cannot expect that all particles on the surface will be bimetallic; formation of monometallic Pd and the second metal and the second metal rich and Pd rich bimetallic particles are more practical from the statistical point of view. The decrease in activity with the addition of a second metal with Pd can be attributed to the decrease in the number of active sites in the bimetallic catalysts compared to the monometallic Pd.

At this point it will be an interesting question to ask whether only the Pd sites are active or the reaction proceeds through a dual site mechanism, which means both the Pd and the second metal participate in the reaction. The following situations can be considered: i. the added second metal is inactive and its only function is to dilute Pd and in the process reduce the number of active Pd ensemble as well as deactivation by coking. ii. the added second metal is also

active in the hydrodehalogenation and coupling reaction along with Pd, which will also act as a source of dissociated hydrogen, which will migrate, to the second metal surface by "spill over" and iii. the Pd ensemble size will become so small that its only function will be to supply dissociated hydrogen to the second metal where all the hydrodehalogenation and coupling reactions will take place. Copper is known to couple the adsorbed alkylidene species formed from geminal alkyldichlorides;[46] Ag catalyzes dimerization of alkyl groups obtained by dissociation of alkyl monohalides.[47-48] Copper and Ag are also known to break C-Cl bonds readily, however, they cannot dissociate H_2 readily.[49] Iron and Co are Fischer-Tropsch catalysts that produce higher molecular weight hydrocarbons from CO and H_2 by coupling hydrocarbon fragments.[50] Also, alumina-supported Co showed hydrodechlorination activity.[51] Therefore, to make any conclusion, one must consider the mechanism of surface alloy formation for all the combinations and their characteristics

Silver and palladium form a continuous series of solid solutions for all bulk compositions, with no documented ordered phases. The surface energies of Ag and Pd are 1.25 and 2 J/m^2, respectively. Considering the significant difference in surface energies, it can be assumed that there will be a significant surface segregation of Ag in the bimetallic Ag-Pd particles. A significant Ag enrichment at the surface (~60% for ~30% bulk Ag content) was reported by Wood and Wise[52] for a commercial alumina-supported Ag/Pd catalyst. Venezia et al. reported a thin layer of Ag particles on top of Pd observed for pumice–supported Pd-Ag catalyst.[53] Numerous other reports[54-57]also suggested segregation of Ag to the surface in Pd-Ag alloy. Looking at the product distribution it can be said that the catalyst property changed significantly by the addition of Ag to Pd. The catalyst Pd-Ag/C produces significant amount of CHF_3 (Figure 5.4b) and C_2F_4 (Figure 5.3b), which were absent for Pd/C. The catalyst also

became inactive within a short time (~40 h). Considering the above factors, it can be speculated that in case of Pd-Ag/C catalyst, there is a very significant amount of bimetallic particle formation and Ag segregates hugely to the surface of the bimetallic particles. The hydrodehalogenation and coupling reactions are occurring over the Ag sites. For the Pd-Cu system, a moderate segregation of Cu to the surface was found.[58-60] So, if one considers a simple model of the surface based on the total Pd-Cu atomic ratio (1:6), there will be less than one Pd atom present per 6 Cu atoms. Based on the model, it can be suggested that the role of Pd in the bimetallic particles will be to dissociate and supply atomic hydrogen to Cu sites; the hydrodehalogenation and coupling activities will occur on Cu sites.

Pd-Co/C showed a very stable catalyst performance though the activity is significantly lower than that of Pd/C. The other interesting thing is to note that no C_{4+} products were detected for Pd-Co/C catalysts. Lower activity can be a result of the site blocking effect of Co. The lack of C_{4+} can be due to the decrease in ensemble size of Pd. Probably formation of longer chain molecules needs bigger ensemble of Pd. Theoretical calculations [61] and experimental results for alumina-supported Pd-Co[62]suggested surface segregation of Pd. Therefore, it can be speculated that the Pd is the only active site and Co acts just to dilute Pd. However, some studies also suggested a change in electronic structure of Pd in the presence of Co.[63-64] The creation of new sites of Pd-Co in the solid solution can change the adsorption strength of the CF_2Cl_2 and hydrocarbons leading to a decrease in activity but to a more stable performance.

The Pd-Fe/C catalyst showed a selectivity pattern that was very similar to Pd/C for all the products except C_{4+}. At the same time the initial activity was approximately half of that of Pd/C. But after ~10 h, the activities for both the catalysts became similar. From these behaviors, it can tentatively be concluded that Fe acts as an inactive Pd site blocking and ensemble size

decreasing element. A huge surface segregation of Pd was observed in various studies.[65-66] The decreasing of the ensemble size might prevent C_{4+} formation as well as catalyst deactivation. This may be the reason why the activity of both Pd/C and Pd-Fe/C become similar after ~10 h. It might be relevant to mention that the catalytic activity of both Pd_5Fe_{95} and Pd_1Fe_{99} for 1,3-butadiene hydrogenation was found comparable to that of pure Pd surface.[66]

5.5 Conclusion

The catalytic behavior of Pd, Pd-Cu, Pd-Ag, Pd-Co and Pd-Fe catalysts supported on activated carbon BPLF3 during the reaction of CF_2Cl_2 and H_2 (250^0C, CFC:H_2=1:1) was investigated to support the hypothesis of involvement of two types of sites for the formation of coupling products. Monometallic Pd produced 75% hydrocarbon oligomerization products (C_2 to C_5) and monometallic Cu, Ag, Co and Fe/C were inactive under the reaction condition. The high selectivity toward hydrocarbons and mainly toward hydrocarbon oligomerization products can be attributed to Pd ensembles of the order of 1-2 nm supported on inert carbon support. Based on the kinetics results the following conclusions have been drawn about the bimetallic catalysts:

For Pd-Ag/C catalyst, there is a very significant amount of bimetallic particle formation and Ag segregates hugely to the surface of the bimetallic particles. The hydrodehalogenation and coupling reactions are occurring over the Ag sites.

For Pd-Cu there will be a moderate surface segregation of Cu to the surface and there will be just enough Pd surface atoms to dissociate hydrogen that migrates to Cu sites for dehalogenation reaction and coupling.

For Pd-Co/Fe, the function of Co is just to dilute the Pd ensemble. For Pd-Fe, Fe acts as Pd site blocking and Pd ensemble size reducing element. Two of the bimetallic catalysts (Pd-Cu and Pd-Co) were very stable though their activities were lower than monometallic Pd.

Table 5.1. Irreversible Gas Uptakes and Apparent Dispersions of Pd-M/C Catalysts

Catalyst composition, wt. %	Uptakes, μmole/g cat				Apparent dispersion, %			
	CO	H_2	O_2	H_2(HT)	CO/Pd_t	H/Pd_t	O/(Pd+M)$_t$	H/Pd_t(HT)
Support	0.0	0.0	3.0	0.0	–	–	–	–
0.5Pd	10.9	0.4	35.8	29.7	21.8	1.5	143.9	119.1
0.47Pd+1.7Cu	0.1	0.2	44.5	33.7	0.3	0.8	202	152.6
0.49Pd+2.92Ag	0.2	0.2	51.7	19.3	0.4	0.8	224	83.6
0.49Pd+1.55Co	7.5	0.2	62.8	35	16.2	1.0	40.6	151.9
0.49Pd+1.46Fe	0	0	62.7	24.6	0	0	40.7	106.9

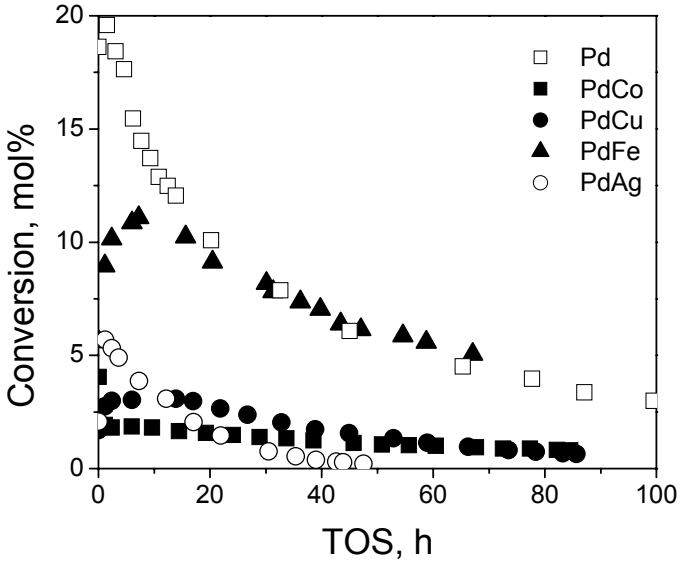

Figure 5.1 Conversion as a function of TOS for Pd/C and Pd-bimetallic catalysts (CF_2Cl_2 :H_2 =1:1 and 523 K).

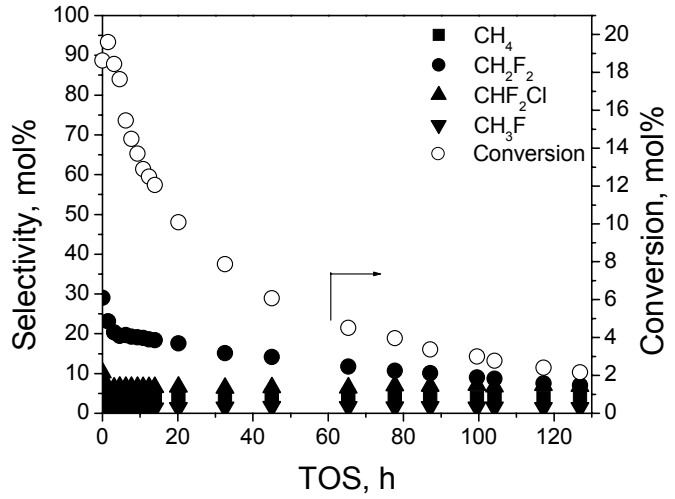

a

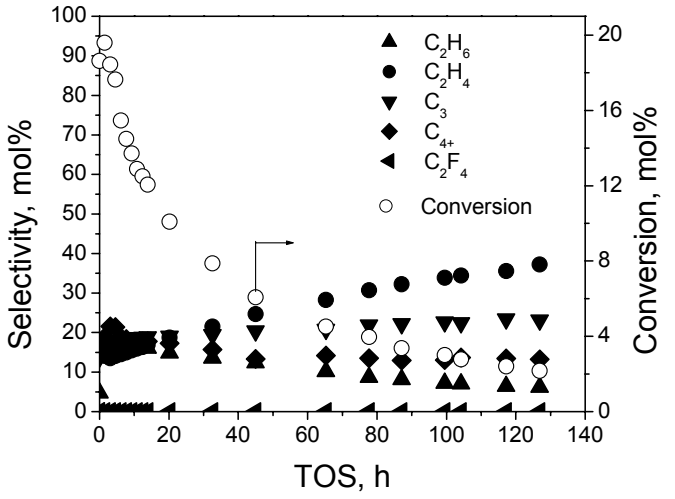

b

Figure 5.2 Selectivity toward C_1 products (a); and coupling products (b) at CF_2Cl_2 : H_2=1:1 and 523 K on Pd/C.

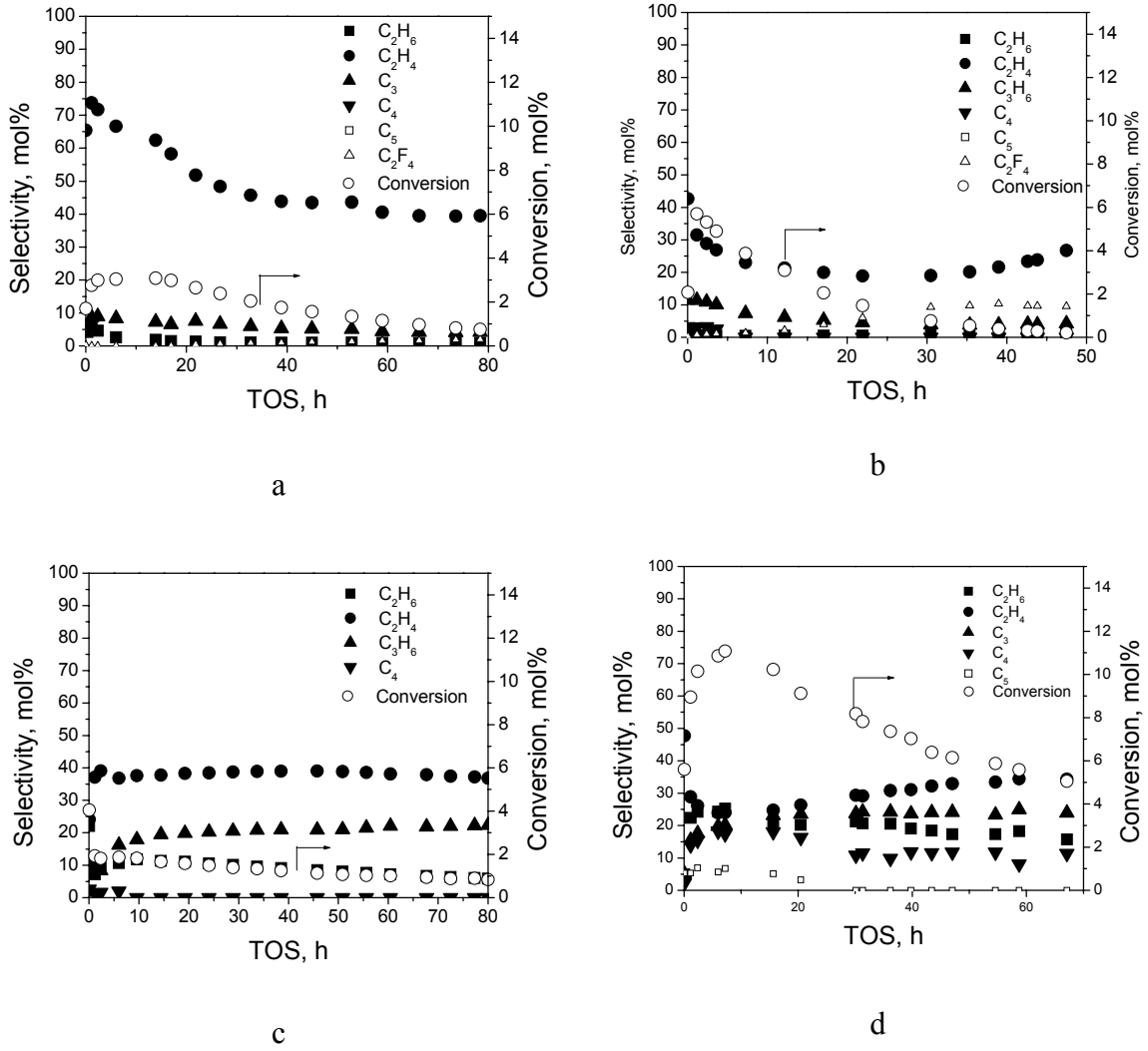

Figure 5.3 Selectivity toward coupling products on Pd-Cu/C (a); Pd-Ag/C(b); Pd-Co/C (c); and Pd-Fe/C (d). at CF_2Cl_2 =1:1 and 523 K

.

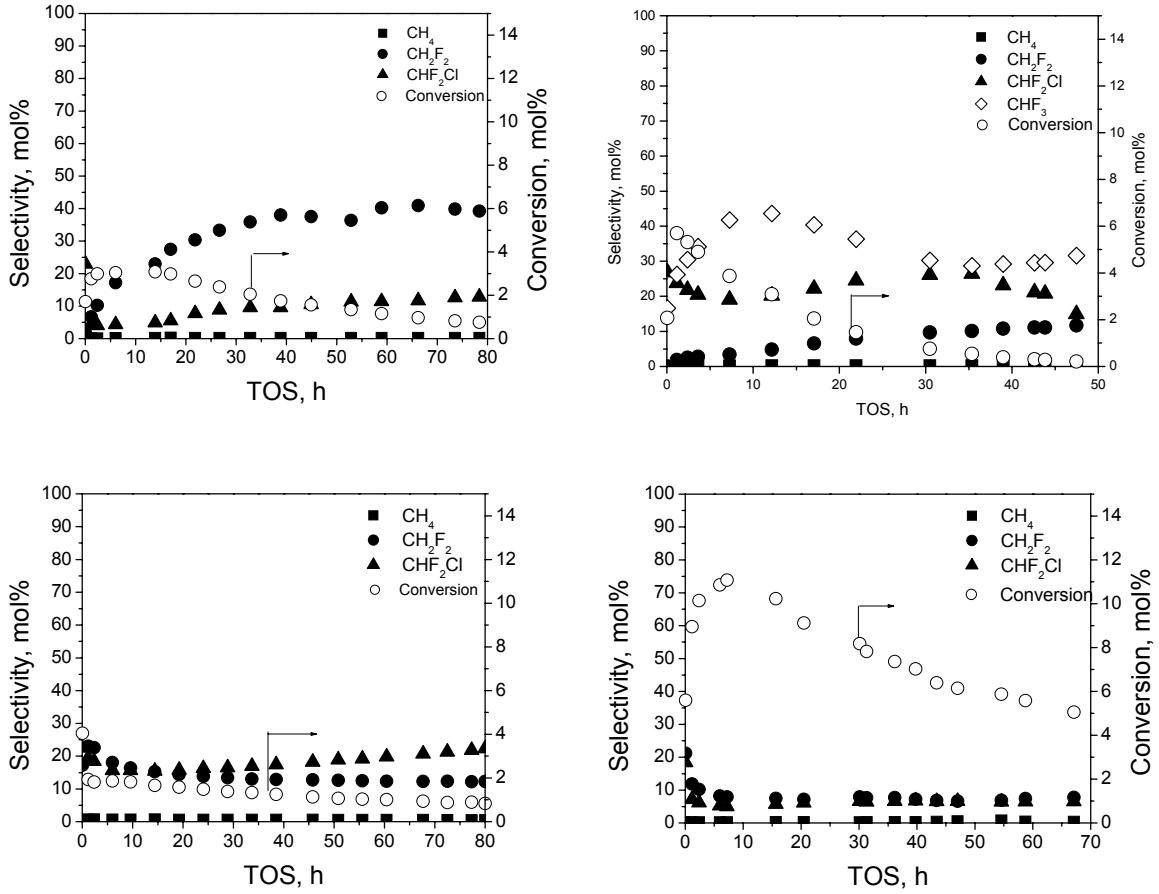

Figure 5.4 Selectivity toward C_1 products on Pd-Cu/C (a); Pd-Ag/C (b); Pd-Co/C (c); and Pd-Fe/C (d) at CF_2Cl_2 =1:1 and 523 K

6.0 SUMMARY AND FUTURE WORK

It has been showed that CF_2Cl_2 can be converted to carbon-carbon coupling products by reacting with H_2 on an appropriate catalyst. Activated carbon has been chosen as the support because of the very corrosive environment of the reaction. The performance of the Pt-Cu/C and Pd-M/C (M=Cu, Ag, Co, Fe) bimetallic catalysts were tested. The main features of the investigation presented in the preceding chapters along with some suggestions for the future investigations are reported here.

6.1 Major Results

The kinetics results of the reaction of CF_2Cl_2 and H_2 catalyzed by PtCu/C catalysts, presented in Chapter 3, showed the effect of Cu content on the selectivity pattern. The observation was that the coupling selectivity increased with the increasing Cu content. The Pt/C catalyst showed less than 5% selectivity toward coupling, whereas

~35% initial selectivity toward hydrocarbon coupling products was observed for Pt1Cu18 (0.5% Pt +2.8% Cu) catalyst. The selectivity pattern changed with TOS. All the catalysts showed an increase in coupling selectivity with TOS. This phenomenon suggests that the modification of the catalytic sites is occurring as the reaction proceeds. It was speculated that the alloy

formation was by the 'catalyzed reduction model'[1] where Pt particles were formed first because of the easy reducibility, and then mobile Cu^{2+} ions were adsorbed by these Pt particles and swiftly reduced. The resulting "cherry" type bimetallic particles consisted of a Pt core and a copper mantle. The TEM micrographs of PtCu/C catalysts after reduction showed the existence of metal particles in the range of 13-30 Å in size and also quasi-spherical particles. Phases of copper oxide was identified in the quasi-spherical particles by electron microdifraction and HREM images. The CuO is most likely the result of exposing the reduced catalyst in air before the TEM studies. As the Cu content in the Pt-Cu catalyst was increased, the size of the copper oxide particles also increased. For example, the size range was 200-500 Å for Pt1Cu9 while for Pt1Cu18 the size was as large as 5000 Å. However, the morphology of the CuO particles was the same for all the Pt-Cu bimetallic samples. This implies that the bimetallic particle formation is not complete after reduction and there are scopes to improve alloy formation by better mixing of the precursors.

The observation that increase of Cu wt% increases coupling during the reaction of CF_2Cl_2 and H_2 led to the investigation of the role of Cu sites in the coupling product formation. Chapter 4 discussed the results of introducing CO in the reaction mixture. The maximum coupling selectivity was increased from 55% to 69%. It was suggested that CO decreases the ensemble sizes of Pt by poisoning the active sites. The catalyst was also exposed to water for better mixing of the precursors. The water-exposed catalyst showed an overall coupling selectivity of 90% and the performance was very stable. It has been suggested that water exposure of the fresh catalyst increases bimetallic particle formation. As a result the number and size of monometallic Pt particles decrease. Both the results point toward the fact that Pt or bimetallic sites may be

responsible for C_1 product formation and Cu sites are responsible for coupling products formation.

The performances of the palladium bimetallic catalysts were discussed in chapter 5. The interesting question was the effect of a second metal on the selectivity pattern of Pd/C catalyst, which was already selective toward coupling product formation in the reaction of CF_2Cl_2 and H_2. The catalytic behavior of Pd, Pd-Cu, Pd-Ag, Pd-Co and Pd-Fe catalysts supported on activated carbon BPLF3 was investigated to support the hypothesis of involvement of two types of sites for the formation of coupling products. Monometallic Pd produced 75% hydrocarbon oligomerization products (C_2 to C_5) and monometallic Cu, Ag, CO and Fe/C were inactive under the reaction condition. The high selectivity toward hydrocarbons and mainly toward hydrocarbon oligomerization products can be attributed to Pd ensembles of the order of 1-2 nm supported on inert carbon. For Pd-Ag/C catalyst, there might be a very significant amount of bimetallic particle formation and Ag segregates hugely to the surface of the bimetallic particles. The hydrodehalogenation and coupling reactions are occurring over the Ag sites. For Pd-Cu there will be a moderate surface segregation of Cu to the surface and there will be just enough Pd surface atoms to dissociate hydrogen to Cu sites for dehalogenation and coupling. For Pd-Co/Fe, the function of Co is just to dilute the Pd ensemble. For Pd-Fe, Fe acts as Pd site blocking and Pd ensemble size reducing element. Two of the bimetallic catalysts (Pd-Cu and Pd-Co) were very stable though their activities were lower than monometallic Pd.

6.2 Future Work

A lot of works remains to be done to understand the fundamental aspects of coupling products formation from CFC hydrodehalogenation, the reasons for changing selectivity pattern and catalyst deactivation with TOS. The following ideas can be pursued in the future:

6.2.1 Studies on PtCu/C Catalyst

Changing selectivity pattern of the bimetallic catalyst with TOS in the reaction of CF_2Cl_2+ H_2 is still a matter of speculation and needs to be addressed in greater detail. Speculations for the changing selectivity pattern are re-dispersion of metallic particles, surface reconstruction and segregation. Surface re-dispersion is a well-established phenomenon in the presence of HCl.[2-4] SiO_2 supported Ni catalyst showed higher Ni particle size after treatment with HCl or HBr.[2] Increase in metal dispersion was observed for tetrachloroethylene hydrodechlorination on carbon supported Pd and Pt.[3] CFCs are also claimed to disperse noble metal catalysts.[5] It is assumed that the mechanism of re-dispersion in the presence of HX (X=Cl, F) involves the formation, volatilization and re-dispersion of unstable metallic halides.[6] This surface re-dispersion process can affect bimetallic particle formation during the course of the reaction and this can be one of the reasons of the changing selectivity of the bimetallic catalysts with TOS. To test the effect, the reduced catalysts can be treated with HCl, HF and the mixture of HCl and HF and then can be characterized by using standard characterization techniques like TEM and XRD. Any difference in particle sizes or bimetallic particle

composition between the reduced catalysts and HX (X=Cl, F) pretreated catalyst will suggest that metal re-dispersion may be one of the reasons for changing catalyst selectivity. Adsorbate induced reconstructions on certain surfaces are extremely common by breaking and making substrate- substrate and /or adsorbate-substrate bonds with substantially altered atomic density in the topmost atomic layer.[7] Extended X-ray absorption fine structure spectroscopy (EXAFS) is very useful to get information about highly dispersed supported bimetallic catalysts with low metal loading.[8] Information about the coordination number and the distance between the atoms can be extracted form EXAFS spectra.[9] In-situ observation of the catalyst state at various TOS by EXAFS can be very useful for a fundamental insight of changing product selectivity with TOS. This experiment will give an understanding about surface reconstruction and segregation as the reaction proceeds.

6.2.2 Studies Using Model Alloy Surfaces

Supports play a big role in the ultimate catalyst performance by changing the geometric and electronic structures of the particles. The particles of Pt or Rh on C or SiO_2 are globular, on Al_2O_3 are hemispherical, while on TiO_2 thin scaly crystals are observed.[10] The absence of support eliminates possible metal-support interactions, so that only the intrinsic catalytic behaviors of the metals are analyzed. To exclude the role of the support, model bimetallic surfaces can be used. Cu can be deposited on Pt (111) to get the model PtCu bimetallic catalyst for CFC hydrodechlorination. Following studies will be useful on the model catalyst.

The average ensemble sizes of Pt and Cu can be determined from a series of STM images[11] after depositing different amounts of Cu on Pt (111). STM images of alloy surfaces

can not only provide topographic information concerning the crystallographic structure but also can show chemical contrast.[12] These model catalysts can be used for CFC hydrodehalogenation. This experiment will give an understanding of the ensemble size requirements of the reaction to form coupling products and will help to find optimum ensemble sizes. In the case of cyclopentane hydrolysis, the highest selectivity toward CH_4 was obtained when the wt% of Re was 80% of the total metal content in Pt-Re/γ AL_2O_3.[13] The striking coefficient of CH_4 on the Au-Ni (111) was shown to be a function of Au coverage and decreased with increasing Au coverage.[11] Similarly, an optimum ensemble size of Pt can be necessary to provide dissociated H_2 and an optimum ensemble size of Cu can be required for producing and coupling carbene radicals from the hydrodehalogenation of CF_2Cl_2.

Coking can be one of the reasons for the changing selectivity of the catalyst with TOS. To test this hypothesis, coke can be deposited on the PtCu model catalyst by C_2H_4 hydrogenation reaction because C_2H_4 preferentially adsorbs on Pt to produce coke[14] and coking occurs at temperatures as low as 300K during C_2H_4 hydrogenation reaction.[15] Copper and other group IB metals are known for their inability to degrade hydrocarbon radicals to produce coke precursors.[16-18] If coking occurs preferentially on Pt sites and the Pt sites get blocked, the selectivity toward the major product CH_4 on Pt would drop and the selectivity toward hydrocarbon coupling products would increase, as Cu atoms are not blocked by coke deposition. This experiment will shed light on the fact if coke deposition is one of the reasons for changing selectivity with TOS.

The speculated reasons for catalyst deactivation are carbonaceous deposits formation and poisoning of active sites by halogen. Performing temperature-programmed reduction (TPR) of

the used model catalyst can be useful to verify the speculation. The following reactions can occur:

$$MX_n + n/2\ H_2 \rightarrow M + n\ HX \quad (M=metal,\ X=Cl,\ F)$$

$$C + 2\ H_2 \rightarrow CH_4$$

Analyzing and quantifying the products of TPD will be useful to determine the reasons of catalyst deactivation during the hydrodehalogenation of CFC.

BIBLIOGRAPHY

BIBLIOGRAPHY

Chapter 1

(1) *Encyclopedia of Chemical Processing and Design*, J.J. Mcketta ed., Marcel Dekker Inc., New york, 1984,Vol.20.

(2) H.H. Saunders and K.C. Frisch, *Polyurethanes Chemistry and Technology*, Part I: Chemistry, Robert E. Krieger Publishing Co., Malabar,Fla., 1962, pp.32.

(3) Krick-Othmer, *Encyclopedia of Chemical Technology*, 3 rd ed., Wiley, New York, 1981, Vol.12.

(4) J. Haggin, Chem. Eng. News, 52 (1981) 59.

(5) P. Pitchai and K. Klier, Catal. Rev. –Sci.Eng., 28 (1986),13.

(6) H.D. Gesser, N.R. Hunter, and C.B. prakash, Chem. Rev., 85 (1985), 235.

(7) N.R. Foster, Appl. Catal., 19 (1985) 1.

(8) R.-S. Liu, M. Iwamoto, and J.H. Lunsford, J. Chem. Soc. Chem. Commun., 78 (1982).

(9) M.M. Khan, and G.A. Somorjai, J. catal., 263 (1985) 91.

(10) M. Iwamoto, Japanese Patent (kokai) 629 (1983) 92.

(11) H.H. Storch, N. Golumbic, and R. B. Anderson, *The Fischer-Tropsch and Related Synthesis*, Wiley, 1951.

(12) *Catalysis*, P.H. Emmett ed., Reinhold, Vol4, 1956

(13) M.A. Vannice, Catalysis Rev., 14 (1976) 153.

(14) V. Ponec, Catalysis Rev., 18(1978) 151

(15) H. Schulz, Appl. Catal. A 186 (1999) 3.

(16) A.A. Adesina, Appl. Catal. A, 345(1996) 138

(17) G.P. van der Laan and A.A.C.M. Beenackers, Catal. Rev.-Science and Engineering, 41 (1999) 255.

(18) J.L.G. Fierro, Catal. Lett. 22 (1993) 67.

(19) R.L. Pruett, Science, 211 (Jan. 2, 1981) 11.

(20) J. H. Lunsford, Catal. Today, 63 (2000) 165.

(21) A. Palermo, J. P. H. Vazquez and R.M. Lambert, Catl. Lett. 68(2000) 191.

(22) S. Pak, P. Qui, and J.H. Lunsford, J. Catal. 179(1998) 222.

(23) P.M. Couwenberg, Q. Chen, and G.B. Marin, Ind. Eng. Chem. Res. 1996 (35) 3999.

(24) A. Palermo, J.P.H. Vazquez, and R.M. Lambert, Catl. Lett., 68 (2000) 191.

(25) G.A. Olah, B. Gupta, M. Farina, J. D. Felberg, W. M. Ip, A. Husain, R. Karpeles, K. Lammertsma, A.K. Melhotra, and N. J. Trivedi, J. Am. Chem. Soc. 107 (1985) 7097.

(26) G.A.Olah, US Patents 4443192, 4465893, 4467130.

(27) G.A. Olah, H. Doggweiler, J.D. Felberg, S. Frahlich, M. J. Grdina, R. Karpeles, T. Keumi, S. Inaba, W.M. Ip, K. Lammertsa, G. Salem, and D.C. Tabor, J. Am. Chem. Soc., 106 (1984), 2143.

(28) H. Stroch, N.G. Golumbic, and R.B. Anderson *,The Fischer-Tropsch and Related Synthesis*, Wiley, 1951

(29) F. Zera, Acc. Chem. Res. 1992 (25) 260 and references therein.

(30) F.Solymosi, K. Revesz, Surf. Sci. 1993 (280) 38.

(31) F.Solymosi, I. Kovacs, Surf. Sci. 1993 (280) 171.

(32) W. Brune, Nature, 379 (1996) 486.

(33) I. Barin, Thermochemical data of pure substances, 3rd Ed. VCH., Weinheim (1995).

(34) P.P. Kulkarni, S.S. Deshmukh, V.I. Kovalchuk, J. L. d'Itri, Catal. Lett. 61 (1999) 161.

(35) P.P. Kulkarni,, V.I. Kovalchuk, J.L. d'Itri, Appl. Catal. B 36 (2002) 299.

(36) B. Coq, S. Hub, F. Figueras and D. Tournigant, Appl. Catal. A 101 (1993) 41.

(37) T. Mori, T. Kikuchi, J. Kubo, and Y. Morikawa, Chem. Lett. 9 (2001) 936.

(38) Y.-C. Hou and C.-M. Chiang, J. Am. Chem. Soc. 1999 (121) 8116.

Chapter 3

(1) W. Brune, Nature, 379 (1996) 486.

(2) Alternative Fluorocarbons Environmental Acceptability Study website (www.afeas.org/production_and_sales.html)

(3) Y.H Choi, and W.Y. Lee, J Mol. Catal. A 193 (2001) 174.

(4) S. Ordonez, F.V. Diez, H. Sastre, Appl. Catal. B 113 (2001) 31.

(5) A.L. Ramos, M. Schmal, D.A.G. Aranda, and G. Somarjai, J.Cata1. 423 (2000) 92

(6) E. J.A.X. Van de Sandt, A. Wiersma, M. Makkee, H.V. Bekkum and J.A. Moulijn, Caltal. Today 35 (1997) 163.

(7) L.S. Vadlamannati, V.I. Kovalchul and J.L. d'Itri, Catal. Lett., 58 (1999) 173.

(8) B. Heinriches, P. Delhez, J. Schoebrechts and J. Pirad, J. Catal.172 (1997) 322.

(9) Y.H Choi, and W.Y. Lee, J Mol. Catal. A 193 (2001) 174.

(10) P.P. Kulkarni, S.S. Deshmukh, V.I Kovalchuk, J.L,d'Itri, Catal. Lett. 61 (1999) 161.

(11) P.P. Kulkarni,, V.I. Kovalchuk, J.L. d'Itri, Appl. Catal. B 36 (2002) 299.

(12) B. Coq, S. Hub, F. Figueras and D. Tournigant, Appl. Catal. A 101 (1993) 41.

(13) J.H. Sinfelt, Bimetallic Catalysts: Discoveries, Concepts, and Applications, Wiley, New York, 1983.

(14) V. Ponec, Applied Catal. A 222 (2001) 31.

(15) P.M. Holmblad, J.H. Larsoen, I. Ckorkendorff, L.P. Nielsen, F. Besenbacher, I. Stensgaard, E. Laegsgaard, P. Kratzer, B. Hammer and J.K. Nørskov, Catal. Lett. 40 (1996) 131.

(16) J.H. Sinfelt, Bimetallic Catalysts: Discoveries, Concepts, and Applications, Wiley, New York, 1983.

(17) V. Ponec, Applied Catal. A 222 (2001) 31.

(18) A.M. Schoeb, T.J. Raeker, L. Yang, T.S. King and A.E. DePristo, Surf. Sci. 278 (1992) L125.

(19) J. A. Rodriguez and D.W. Goodman, Science 257 (1992) 897.

(20) P.M. Holmblad, J.H. Larsoen, I. Ckorkendorff, L.P. Nielsen, F. Besenbacher, I. Stensgaard, E. Laegsgaard, P. Kratzer, B. Hammer and J.K. Nørskov, Catal. Lett. 40 (1996) 131.

(21) P.P. Kulkarni, V.I. Kovalchuk, J.L. d'Itri, Appl. Catal. B 36 (2002) 299.

(22) J.R. Anderson, Structure of Metallic Catalysts, Academic Press, London, 1975, Chapter 6.

(23) K.O. Early, W.D. Rhodes, V.I. Kovalchuk, J.L. d'Itri, Appl. Catal. 26 (2000) 257.

(24) D.H. Ann, J.S. Lee, M. Nomura, W.M. Sachtler, G. Moretti, S.I. Woo, and R. Ryoo, J. Catal. 133 (1992) 191.

(25) S. Horch, H.T. Lorensen, S. Helveg, E. Laegsgaard, I. Stensgaard, K.W. Jacobsen, J.K. Nørskov and F. Besenbacher, Nature, 398 (1999), 134.

(26) U. Schroder, R. Linke, J.-H. Boo, K. Wandelt , Surf. Sci., 352-354 (1996) 211.

(27) Y.G. Shen, D.J. O'Connor, K. Wandelt, and R.J. MacDonald, Surf. Sci. 331-333 (1995) 746.

(28) B.Coq, G.Ferrat, and F. Figueras, J. Catal. 101 (1986).

(29) B. Coq, G. Ferrat, and R. Figueras, React. Kinet. Catal. Lett. 27 (1985) 157.

(30) P. Fouilloux, G. Cordier and Y. Colleuille, Stud. Surf. Sci. Catal. 11 (1982) 369.

(31) Obuchi, A. Ogata , K. Mizuno, A. Ohi, H. Ohuchi , Collids and Surfaces A 80 (1993) 121.

(32) M. X. Yang, S. Sarkar, and B. E. Bent, Langmuir 13 (1997) 229.

(33) Jose A. Rodriguez,Surf. Sci. Reports 24 (1996) 223.

(34) A .L. Ramos, M. Schmal, D.A.G. Aranda, and G. Somarjai, J.Cata1. 423 (2000) 92

(35) Y. Hou, and C. Ching , J. Am. Chem. Soc. 121 (1999) 8116

(36) S. Deshmukh and J.L. d'Itri, Catal. Today 40 (1998) 377.

(37) J. W. Bozzelli, Y.-M. Chen, and S.S.C. chuang, Chem Eng. Commm., 115 (1992) 1.

(38) C.D. Thompson, R. M. Rioux, N. Chen, and F. H. Ribeiro, J. Phys. Chem. B 104 (2000) 3067

(39) S. Ordonez, F. V. Diez, and H. Sastre, Appl. Catal. B, 31 (2001) 113.

(40) Wiersma, E. J.A.X. van de Sandt, M. A. den Hollander, H. van Bekkum, M.Makkee,and J. A. Moulijn, J. Calal. 177 (1998) 29.

Chapter 4

(1) S. Ordonez, F.V. Diez, H. Sastre, Appl. Catal. B 113 (2001) 3.

(2) A.L. Ramos, M. Schmal, D.A.G. Aranda, and G. Somarjai, J.Cata1. 423 (2000) 92.

(3) E. J.A.X. Van de Sandt, A. Wiersma, M. Makkee, H.V. Bekkum and J.A. Moulijn, Caltal. Today 35 (1997) 163.

(4) L.S. Vadlamannati, V.I. Kovalchul and J.L. d'Itri, Catal. Lett., 58 (1999) 173.

(5) B. Heinriches, P. Delhez, J. Schoebrechts and J. Pirad, J. Catal.172 (1997) 322.

(6) Y.H Choi, and W.Y. Lee, J Mol. Catal. A 193 (2001) 174.

(7) P.P. Kulkarni,, V.I. Kovalchuk, J.L. d'Itri, Appl. Catal. B 36 (2002) 299.

(8) B.Coq, G.Ferrat, and F. Figueras, J. Catal. 101 (1986).

(9) B. Coq, G. Ferrat, and R. Figueras, React. Kinet. Catal. Lett. 27 (1985) 157.

(10) P. Fouilloux, G. Cordier and Y. Colleuille, Stud. Surf. Sci. Catal. 11 (1982) 369.

(11) B. Coq, S. Hub, F. Giguéras, and D. Tournigant, Appl. Catal. A 101 (1993) 41.

(12) R. Linke, U. Schneider, H. Busse, C. Becker, U. Schroder, G.R. Castro, K. Wandelt, Surf. Sci. 307 (1994) 407.

(13) P.N. Ross and P. Stonehart, J. Catal. 35 (1974) 391.

(14) G.A. Somorjai, *Introduction to Surface Chemistry and Catalysis*, Wiley, New York, 1994.

(15) P.P. Kulkarni, V.I. Kovalchuk, J.L. d'Itri, Appl. Catal. B 36 (1999) 299.

(16) N.M. Markovic, P.N. Ross Jr. , Surface Science Reports, 45 (2002) 117.

(17) D.H. Ann, J.S. Lee, M. Nomura, W.M. Sachtler, G. Moretti, S.I. Woo, and R. Ryoo, J. Catal. 133 (1992) 191.

(18) Z. Zhang, W.M.H. Scahtler, and S.L. Suib, Catal. Lett. 2 (1989) 395.

(19) Z. Zhang and W.M.H. Scahtler, J. Chem. Soc, Faraday Trans. 86 (1990) 2312.

(20) J.S. Feeley, and W.M.H. Scahtler, Zeolites 10 (1990) 738.

(21) F.B. Noronha, M. Schmal, R. Frety, G. Bergeret, and B. Moraweck, J. Catal. 186 (1999) 20.

(22) H. Idriss, C. Diagne, J.P. Hindermann, A. Kinnemann, and M.A. Barteau, in "Proceedings, 10 th International Congress on Catalysis, Budapest, 1992" (L. Guczi, F. Solymosi, and P. Tetenyi, Eds.) , part C, p.2119, Elsevier, Budapest, 1992.

(23) M.P. Kapoor, A.L. Lapidus, and Krylova, in "Proceedings, 10 th International Congress on Catalysis, Budapest, 1992" (L. Guczi, F. Solymosi, and P. Tetenyi, Eds.) , part C, p.2119, Elsevier, Budapest, 1992.

(24) W. Juszczyk, Z. Karpinski, D. Lomot, J. Pielaszek, Z. Paal, and A.Y.Stakheev, J. Catal. 142 (1993) 617.

(25) F.B. Noronha, M. Schmal, C. Nicot, B. Moraweck, and R. Frety, J. Catal. 168 (1997) 42.

(26) Y.-G. Yin, Z. Zhang, and W. M. H. Sachtler, J. Catal. 139 (1993) 444.

(27) P. P. Kulkarni, V. I. Kovalchuk, J.L. d'itri, Appl. Catal. B 36 (2002) 299.

(28) D. Chakraborty, P. P. Kulkarni, V. I. Kovalchuk, J.L. d'itri, manuscript in preparation.

(29) S. Ordonez, F. V. Diez, and H. Sastre, Appl. Catal. B, 31 (2001) 113.

(30) M. X. Yang, S. Sarkar, and B. E. Bent, Langmuir 13 (1997) 229.

Chapter 5

(1) G.A. Olah, B. Gupta, M. Farina, J. D. Felberg, W. M. Ip, A. Husain, R. Karpeles, K. Lammertsma, A.K. Melhotra, and N. J. Trivedi, J. Am. Chem. Soc. 107 (1985) 7097

(2) G.A.Olah, US Patents 4443192, 4465893, 4467130.

(3) G.A. Olah, H. Doggweiler, J.D. Felberg, S. Frahlich, M. J. Grdina, R. Karpeles, T. Keumi, S. Inaba, W.M. Ip, K. Lammertsa, G. Salem, and D.C. Tabor, J. Am. Chem. Soc., 106 (1984), 2143.

(4) W. Brune, Nature, 379 (1996) 486.

(5) E.J.A.X. van de Sandt, A. Wiersma, M. Makkee, H. van Bekkum and J.A. Moulijn, Appl. Catal. A , 155 (1997) 57.

(6) B. Coq, J.M. Cognion, F. Figueras, and D. Tornigant, J. Catal., 141 (1993) 21.

(7) K. O. Early, V.I. Kovalchuk, F. Lonyi, S.S. Deshmukh, and J. L. d'Itri, J. Catal., 182 (1999) 219.

(8) Z. Ainbinder, L.E. Manzer, and M.J. Nappa, in Environmental Catalysis (Edited by G. Ertl, H. Knozinger, and J. Weitkamp), Wiley-VCH, New York, 1999, 197.

(9) S.Y. Kim, H.C. Choi, O.B. Yanga, K.H. Lee, J.S. Lee, Y.G. Kim, J. Chem. Soc., Chem. Commun., (1995) 2169.

(10) A. Wiersma, E.J.A.X. van de Sandt, M. Makkee, C.P. Luteijn, H. van Bekkum, and J. A. Moulijn, Catal. Today, 27 (1996)257.

(11) A. Wiersma, E.J.A.X. van de Sandt, M.A. den Hollander, H. van Bekkum, M. Makkee, and J.A. Moulijn, J. Catal., 177 (1998) 29.

(12) T. Mori, W. Ueda, Y. Morikawa, Catal. Lett. 38 (1996) 73.

(13) A. D. Harley, M.T. Holbrooks, S.R. Bare, and J.L. Womack, 14th Meeting of the North American Catalysis Society, Snowbird, Utah, 1995.

(14) W. A. A. van Barneveld, V. Ponec, J. Catal. 88 (1984) 382.

(15) A. H. Weiss, S. Valinski, G.V. Antoshin, J. Catal., 74 (1982) 136.

(16) P.P. Kulkarni, S.S. Deshmukh, V.I Kovalchuk, and J.L. d'Itri, Catal. Lett. 61 (1999) 161.

(17) J.H. Sinfelt, *Bimetallic Catalysts: Discoveries, Concepts, and Applications,* Wiley, New York, 1983.

(18) V. Ponec, Applied Catal. A 222 (2001) 31.

(19) P.M. Holmblad, J.H. Larsoen, I. Ckorkendorff, L.P. Nielsen, F. Besenbacher, I. Stensgaard, E. Laegsgaard, P. Kratzer, B. Hammer and J.K. Nørskov, Catal. Lett. 40 (1996) 131.

(20) J.H. Sinfelt, *Bimetallic Catalysts: Discoveries, Concepts, and Applications,* Wiley, New York, 1983.

(21) V. Ponec, Applied Catal. A 222 (2001) 31.

(22) A.M. Schoeb, T.J. Raeker, L. Yang, T.S. King and A.E. DePristo, Surf. Sci. 278 (1992) L125.

(23) J. A. Rodriguez and D.W. Goodman, Science 257 (1992) 897.

(24) P.P. Kulkarni, V.I. Kovalchuk, J.L. d'Itri, Appl. Catal. B 36 (2002) 299.

(25) B. Coq, S. Hub, F. Figueras and D. Tournigant, Appl. Catal. A 101 (1993) 41.

(26) A. Morato, C. Alonso, F. Medina, P. Salagre, J.E. Sueiras, R. Terrado, A. Giralt, Appl. Catal. B 23 (1999) 175.

(27) S.C. Fang and J.H. Sinfelt, J. Catal., 103 (1987) 220.

(28) A. Paul and B.E. Bent, J. Catal., 147 (1994) 264.

(29) M.X. Yang, S. Sarkar, B.E. Bent, S.R. Bare, and M.T. Holbrook, Langmuir, 13 (1997) 229.

(30) J.R. Anderson, *Structure of Metallic Catalysts*, Academic Press, London, 1975, Chapter 6.

(31) H. Stroch, N.G. Golumbic, and R.B. Anderson, The Fischer-Tropsch and Related Synthesis, Wiley, New York, 1951.

(32) B.Coq, G.Ferrat, and F. Figueras, J. Catal. 101 (1986).

(33) B. Coq, G. Ferrat, and R. Figueras, React. Kinet. Catal. Lett. 27 (1985) 157.

(34) P. Fouilloux, G. Cordier and Y. Colleuille, Stud. Surf. Sci. Catal. 11 (1982) 369.

(35) B. Coq, S. Hub, F. Figueras and D. Tournigant, Appl. Catal. A 101 (1993) 41.

(36) A. Wiersma, E. J. A. X. van de Sandt, M.A. den Hollander, H. van Bekkum, M. Makkee, J. A. Moulijn, J. Catal., 177 (1998) 29.

(37) Karpinski et al., Appl. Catal A. 166 (1998) 311.

(38) K. Early, V. I. Kovalchuk, F. Lonyi, S. Deshmukh, J. L. d'Itri, J. Catal., 182 (1999) 219.

(39) F.J. Urbano, J.M. Marinas, J. Mol. Catal. A 173 (2001) 329

(40) P. N. Rylander, Catalytic Hydrogenation in Organic Synthesis, Academic Press, San Diego, 1979.

(41) Z. Ainbinder, L.E. Manzer,, M.J. Nappa, in : G. Ertl, H. Knozinger, J. Weitkamp (Eds.), handbook of Heterogeneous Catalysis, Vol. 4, Wiley-VCH, Weinheim, 1997, p. 1677.

(42) B. Coq, F. Figueras, S. Hub, D. Tornigant, J. Phys. Chem. 99 (1995) 11159.

(43) Juszczyk, A. Malinowski, and Z. Karpinski, Appl. Catal. A 166 (1998) 311.

(44) E.S. Lokteva, V.V. Lunin, E.V. Golubina, V.I. Simagina, M. Egorova, I.V. Stoyanova, Stud. Surf. Sci. Catal., 130 (2000) 1997.

(45) D.H. Ann, J.S. Lee, M. Nomura, W.M. Sachtler, G. Moretti, S.I. Woo, and R. Ryoo, J. Catal. 133 (1992) 191.

(46) Yang, M. X., Sarkar, S., Bent, B. E., Bare, S. R., and Holbrook, M. T., Langmuir, 13 (1997) 229.

(47) Zhou X.-L., and White, J. M., J. Phys. Chem., 95 (1991) 5575.

(48) Zhou, X.-L., Schwaner, A. L., and White, J. M., J. Am. Chem. Soc., 115 (1993) 4309.

(49) Fung, S. C., and Sinfelt, J. H., J. Catal., 103 (1987) 220.

(50) Storch, H., Golumbic, N. G., and Anderson, R. B., The Fischer-Tropsch and Related Syntheses, Wiley: New York, 1951.

(51) I.V. Mishalov, V.V. Chesnokov, R.A. Buyanov, and N.A. Pakhomov, Kinetics and Catalysis, 42 (20010 543.

(52) B.J. Wood and H. Wise, Surf. Sci. 52 (1975) 151.

(53) A.M. Venezia, L. F. Liotta, G. Deganello, Z. Schay, and L. Guczi, J. Catal., 182 (19990 449.

(54) E.G. Allison, G.C. Bond, Catal. Rev. 7 (1972) 233.

(55) G.P. Schwartz, Surf. Sci. 76 (1978) 113.

(56) F.J. Kuijers and V. Ponec, J. Catal. 60 (1979) 100.

(57) M. Yamamura, K. Kaneda, and T. Imanaka, Catal. Lett. 3 (1998) 203.

(58) F. Reniers, M.P. Delplencke, A. Askali, A. Jardinier-Offergeld, F. Bouillon, Appl. Surf. Sci. 81 (1994) 151.

(59) A.D. van Langeveld, H.A.C.M. Hendrickx, B.E. Nieuwenhuys, Thin Solid Films 109 (1983) 179.

(60) J.A. Anderson and M. Fernandez-Garcia, Trans IChemE, 78 (2000) 935.

(61) P. M. Ossi, Surf. Sci. 201 (1988) L519.

(62) Juszczyk, W., Z. Karpiniski, D. Lomot, J. Pielaszek, Z. Paal,, and A.Y. Stakheev, J. Catal., 60 (1993) 617.

(63) F.B. Noronha, M. Schmal, R. Frety, G. Bergeret, and B. Moraweck, J. Catal. , 186 (1999) 20.

(64) A. Sarkany, Z. Zsoldos, B. Furlong, J.W. Hightower, and L. Guczi, J. Catal. 141 (1993) 566.

(65) I. Meunier, J.M. Gay, L. Lapena, B. Aufray, H. Oughaddou, E. Landemark, G. Falkenberg, L. Lottermoser, and R.L. Johnson, Surf. Sci. 42 (1999) 422.

(66) J.C. Bertoline, J.L. Rousset, P. Miegge, J. Massardier, B. Tardy, Y. Samson, B.C. Khanra, and C. Cremers, Surf. Sci. 102 (1993) 281.

Chapter 6

(1) D.H. Ann, J.S. Lee, M. Nomura, W.M. Sachtler, G. Moretti, S.I. Woo, and R. Ryoo, J. Catal. 133 1992) 191.

(2) C. Menini, C. Park, E.-J. Shin, G. Tavoularis, and M. A. Keane, Catal. Today 62 (2000) 355.

(3) S. Ordonez, F. V. Diez, H. Sastre, Appl. Catal. B 31 (2001) 113.

(4) C. Menini, C. Park, E.-J. Shin, and M. A. Keane, J. Phys. Chem. B, 104 (2000).

(5) C.S. Kellner, J.J. Lerou, V. Rao, and K.G. Wuttke, Regeneration or activation of noble metal catalysts using fluorohalocarbons or fluorohalohydrocarbons, World Pat. Appl. WO 91/04097 to Du Pont de Nemours and company (1991).

(6) K. Foger, D. Hay, H. Jaeger, J. Catal. 96 (1985) 154.

(7) G. A. Somorjai, M.A. Van Hove, Prog. Surf. Sci. 40 (1998) 201.

(8) L. Guczi, D. Bazin, Z. Schay, and I. Kovacs, Surf. Interface anal. 34 (2002), 72.

(9) G. Berlier, G. Spoto, P. Fisicaro, S. Bordiga, A. Zecchina, E. Giamello, and C. Lamberti, Microchemical Journal 71 (2002) 101.

(10) M. Shpiro, *Catalyst Surface: Physical Methods of Studying,* Mir Publishers, Moscow, 2000, Chapter 4.

(11) P.M. Holmblad, J. H. Larsen, I. Chorkendorff, L. P. Nielsen, F. Besenbacher, I. Stensgaard, E. Laegsgaard, P. Kartzer, B. Hammer, and J.K. Norskov, Catal. Lett. 40 (1996) 131.

(12) P. Varga and M. Schmid, Appl. Surf. Sci. 141 (1999) 287.

(13) C. L. Pieck, P. Marecot, J.M. Parera, J. Barbier, Appl. Catal. A 126 (1995) 153.

(14) A.D. van Langeveld, F.C.M.J. van Delft and V. Ponc, Surf. Sci., 134 (1983) 665.

(15) M. Masi, M. Sangalli, S. Carra, G. Cao, and M. Morbidelli, Chem. Eng. Sci., 43 (1988) 1849.

(16) A. Paul and B.E. Bent, J. Catal., 147 (1994) 264.

(17) M.X. Yang, S. Sarkar, B.E. Bent, S.R. Bare and M.T. Holbrook, Langmuir, 13 (1997) 229.

(18) C.-M. Ching, T.H. Wentzlaff and B.E. Bent, J. Phys. Chem., 96 (1992) 1836.